ENC 2012
EUROPEAN NUCLEAR CONFERENCE

Transactions - Life Sciences Non-Power Applications

EUROPEAN NUCLEAR SOCIETY

ENS CONFERENCE

ENC 2012 Diamond Sponsor:

HITACHI

ENC 2012 Gold Sponsors:

AGORIA
no future without technology

Belgoprocess

SCK·CEN
STUDIECENTRUM VOOR KERNENERGIE
CENTRE D'ETUDE DE L'ENERGIE NUCLEAIRE

NUCLEAIR FORUM NUCLEAIRE

ENC 2012 Silver Sponsor:

urenco

ENC 2012 Sponsor:

ONET TECHNOLOGIES

organised in collaboration with:

the Nuclear Institute

IAEA International Atomic Energy Agency

NEA Nuclear Energy Agency

European Nuclear Society
Rue Belliard 65
1040 Brussels, Belgium
Phone + 32 2 505 30 54
Fax +32 2 502 39 02
E-mail ens@euronuclear.org
Internet www.euronuclear.org

ISBN 978-92-95064-14-0

These transactions contain all contributions submitted by 7 December 2012.

OECD-NUCLEAR ENERGY AGENCY'S APPROACH FOR A RELIABLE SUPPLY OF MOLYBDENUM-99 AND TECHNETIUM-99M	Cameron, R. (1); Westmacott, C. (1); Peykov, P. (1) 1 - Nuclear Development Division, OECD – Nuclear Energy Agency, France
Thyroid Doses Received by the Public of Belarus due to the Fukushima-Daiichi Nuclear Accident	Kenigsberg, J. (1); Kouts, K. (2) 1 - National Commission on Radiation Protection under the Council of Ministers of the Republic of Belarus, Belarus 2 - Republican Scientific-Practical Center of Hygiene, Belarus
Predictive model of aerosol transport and deposition. Application and validation to the PWR reactor building	Mohand-Kaci, H. (1); Ricciardi, L. (1); Jahan, S. (2); Lestang, M. (3) 1 - IRSN DSU/SERAC, France 2 - EDF R&D STEP, France 3 - EDF DPN/UNIE, France
Carbon ion irradiation suppresses metastasis related genes in human prostate carcinoma cells.	Suetens, A. (1); Moreels, M. (1); Tabury, K. (1); Quintens, R. (1); D'Agostino, E. (2); Baatout, S. (1); Deconinck, F. (1) 1 - Radiobiology Unit, Belgian Nuclear Research Centre, SCK•CEN, Boeretang 200, 2400 Mol, Belgium, Belgium 2 - Radiation protection, Dosimetry and Calibration Unit, Belgian Nuclear Research Centre, SCK•CEN, Boeretang 200, 2400 Mol,, Belgium
RESEARCH REACTOR CONTRIBUTIONS TO RENEWABLE ENERGY SOLUTIONS	Van Walle, D. E. (1) 1 - SCK•CEN, Belgium
Sellafield dose impacts on non-human biota	Mcdonald, P. (1); Copplestone, D. (2); Lutman, E. (1); Humak, S. (1); Stevens, A. (3) 1 - AMEC, Innovation Centre, Westlakes Science and Technology Park, Moor Row, Cumbria CA24 3TP, United kingdom 2 - Biological & Environmental Sciences, School of Natural Sciences, University of Stirling, Stirling, FK9 4LA, United kingdom 3 - Sellafield Ltd, Sellafield, Seascale, Cumbria CA20 1PG, United kingdom
Chronic exposure to simulated space conditions affects gene expression in mouse fetal fibroblasts	Beck, M. (1); Moreels, M. (1); Quintens, R. (1); Abou-el-ardat1, K. (1); Tabury, K. (1); Michaux, A. (1); Janssen, A. (1); Neefs, M. (1); Van oostveldt, P. (2); De vos, W. (2); Baatout, S. (1) 1 - Radiobiology Unit, Belgian Nuclear Research Centre, SCK•CEN, Boeretang 200, 2400 Mol, Belgium 2 - Department for Molecular Biotechnology / NB photonics, Ghent University, Ghent, Belgium

LIFE SCIENCES AND NON-POWER APPLICATIONS

THE HIGH-LEVEL GROUP ON THE SECURITY OF SUPPLY OF MEDICAL RADIOISOTOPES: POLICY APPROACH AND ITS IMPLEMENTATION

Ron Cameron, Pavel Peykov and Chad Westmacott

OECD Nuclear Energy Agency
Issy les Moulineaux
92130 France

Abstract

Following the major shortages of the vital medical isotope molybdenum-99 (^{99}Mo) and its decay product, technetium-99m (^{99m}Tc), in 2009-2010, the OECD Nuclear Energy Agency (NEA), through its High-level Group on the Security of Supply of Medical Radioisotopes (HLG-MR), examined the reasons for the market failure that led to a lack of security of supply of ^{99}Mo/^{99m}Tc and developed a policy approach to address the challenges to reliable supply. This paper describes those challenges and the policy approach to ensure a long-term secure supply of this important nuclear diagnostic agent for patients. The policy approach includes ways to send strong price signals across the supply chain, ensuring international co-ordination of supply availability, improving communication and demand side management and establishing a mechanism for reviewing its implementation. The paper also describes how multipurpose irradiators can implement full-cost recovery, a necessary change for encouraging the investment in new infrastructure needed to secure global supply. The paper will also discuss the ongoing work of the HLG-MR, focusing on: a) the implementation of the policy approach by all producing and consuming countries and, b) examining the cost and supply impacts of converting to ^{99}Mo produced from low enriched uranium targets. It will briefly present the economic and capacity models of the supply chain and the results of the analysis, showing the impact of conversion on the costs and availability of ^{99}Mo in the supply chain, and identify policy options to ensure a reliable supply of ^{99}Mo/^{99m}Tc during and after the transition to using low enriched uranium targets for ^{99}Mo production.

1. Introduction

The major shortages of key medical radioisotopes molybdenum-99 (^{99}Mo) and its decay product, technetium-99m (^{99m}Tc), focused attention on the global supply chain for these isotopes and led to the creation of the High-level Group on the Security of Supply of Medical Radioisotopes (HLG-MR). Since 2009, this group has identified the reasons for the isotope shortages and developed a policy approach to address the challenges to a long-term secure supply of these important isotopes.

Through its comprehensive research and analysis of the ^{99}Mo/^{99m}Tc supply chain to date, the HLG-MR has articulated the “central pillars” of reform needed for a sustainable industry in the long term. These pillars recognise the current challenges faced by stakeholders and represent the key high-level actions that the policy approach seeks to encourage. The central pillars are:

- Market economics in the ^{99}Mo/^{99m}Tc supply chain need to be improved.
- Structural changes are necessary (e.g. diversity of supply).
- The government role in the production of these key isotopes has to be clearly defined.
- An effective, co-ordinated international approach is necessary.

The central pillars of the HLG-MR policy approach have been further refined into policy principles with supporting recommendations. Implementing these policy principles by all government and industry stakeholders is critical for ensuring the long-term reliability of $^{99}Mo/^{99m}Tc$ supply.

In addition to the ongoing concerns related to long-term reliability, all current major ^{99}Mo-producing nations have agreed to convert to using low-enriched uranium (LEU) targets for the production of ^{99}Mo. This decision is based on important non-proliferation reasons; however, the conversion will have potential impacts on the global supply chain, both in terms of costs and available capacity.

It is also important to note that global access to a stable and secure supply of highly enriched uranium (HEU) for $^{99}Mo/^{99m}Tc$ production may be severely restricted or completely eliminated in the mid-term[1]. As a result, long-term security of supply of these important medical isotopes requires the move to non-HEU-based production through conversion to LEU targets for ^{99}Mo production in existing (and new) producers, and through the use of alternative technologies.

Recognising this situation, the NEA and its HLG-MR undertook a study to quantify the expected capacity and cost impacts of LEU-target conversion. The study also identified potential policy options to ensure a reliable supply of $^{99}Mo/^{99m}Tc$ produced without HEU, consistent with the timeframes and policies of the HLG-MR.

2. The HLG-MR Policy Approach

Under its first mandate (June 2009-2011), the HLG-MR examined the major issues that affect the short-, medium- and long-term reliability of $^{99}Mo/^{99m}Tc$ supply and developed a policy approach to move the supply chain to a sustainable basis and ensure security of supply. The policy approach includes six principles[2], along with supporting recommendations[3].

The objectives of the HLG-MR during its second mandate (July 2011-2013) are to work towards increasing the long-term security of supply of $^{99}Mo/^{99m}Tc$ through the implementation of the HLG-MR policy approach. This entails actions to maintain transparency on global developments, continue communication with the supply chain and end users, evaluate progress toward implementation, and provide additional information and analysis where necessary. A key action under the second mandate is to provide guidance in areas critical for achieving long-term economic sustainability in the market, e.g. full-cost recovery and outage reserve capacity.

Full-cost Recovery

The NEA has developed a guidance document on full-cost recovery to assist reactor and alternative production technology (e.g., cyclotrons, accelerators) operators on how to undertake

[1] For example, the American Medical Isotopes Production Act of 2011 (S.99), which has passed the US Senate and was in front of the US House of Representatives at the time of writing, includes provisions to restrict the export of HEU from the United States for the purposes of medical isotope production, seven years after enactment.

[2] The six policy principles relate to:

- the implementation of full-cost recovery throughout the $^{99}Mo/^{99m}Tc$ supply chain;
- the provision of and payment for reserve capacity by the supply chain;
- the role of governments in establishing rules for the proper functioning of the market, without direct intervention;
- the provision of support by governments to reactors and processors to facilitate the conversion of ^{99}Mo-producing facilities to the use of non-HEU;
- continuous international collaboration; and,
- performance of periodic assessments of the supply chain to ensure progress towards the implementation of the HLG-MR policy approach.

[3] A full discussion of the supporting recommendations is presented in *The Supply of Medical Radioisotopes: the Path to Reliability* (OECD-NEA, 2011).

full-cost identification and implement full-cost recovery[4]. The document also discusses issues related to levelling the playing field between old and new reactors.

The guidance document is based on the policy principle relating to full-cost recovery. This principle follows the findings of the OECD/NEA report, *The Supply of Medical Radioisotopes: An Economic Study of The Molybdenum-99 Supply Chain* (NEA, 2010), which clearly demonstrated that the pricing structure from reactors for ^{99}Mo irradiation services prior to the 2009-2010 supply shortages was not economically sustainable, with the cost being subsidised by host nations. The governments of these nations have indicated a move away from subsidising production, which often benefits foreign nations or foreign companies, and therefore pricing for the irradiation services must recover the full cost of production to ensure economic sustainability and a long-term secure supply. Appropriate pricing would also encourage more efficient use of ^{99}Mo/^{99m}Tc, reducing excess production and the associated radioactive waste.

Figure 1. Full-cost recovery: High-level cost elements

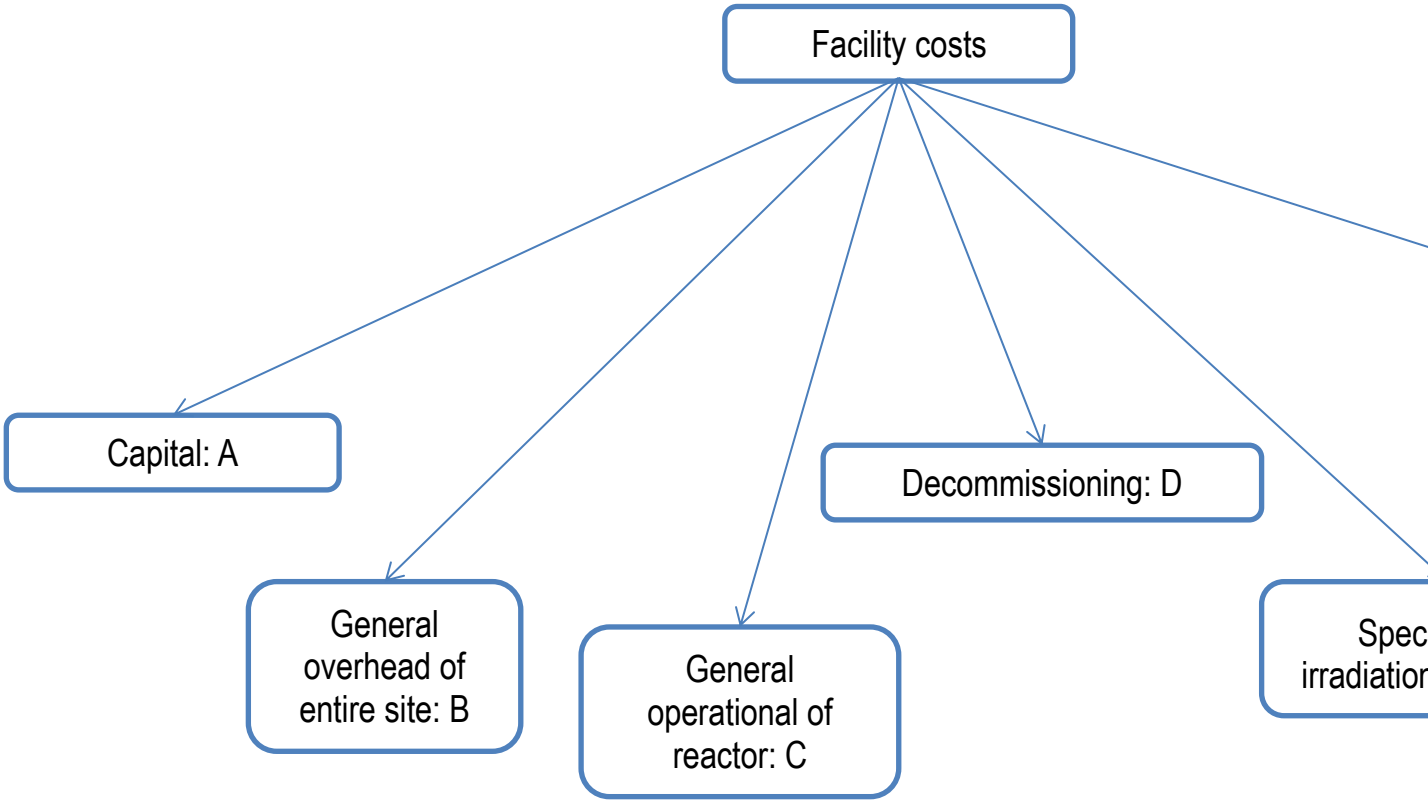

Full Cost of ^{99}Mo = wA + y(xB + C)+ zD + E,

where:

wA = the portion of capital costs attributable to ^{99}Mo irradiation services;
xB = the portion of overhead costs attributable to all reactor operations[5];
yxB = the portion of operational costs attributable specifically to ^{99}Mo irradiation services; and,
zD = the portion of decommissioning costs attributable to ^{99}Mo irradiation services.
E = direct costs for target irradiations

[4] Available at: http://oecd-nea.org/med-radio/guidance/

[5] Excludes the overhead costs attributable to facility operations not related to ^{99}Mo, e.g. laboratory activities.

Implementation of full-cost identification and recovery by traditional multi-purpose research reactors and other $^{99}Mo/^{99m}Tc$ production technologies will provide the economic incentives to develop and invest in future ^{99}Mo-related infrastructure and to fully pay operating costs. For a consistent approach on how costs are identified, the NEA guidance document provides a full-cost recovery methodology that identifies the essential elements to be included when determining the full-cost of ^{99}Mo irradiation services, including a reasonable portion of facility common costs, and how these elements should be allocated among various missions in multipurpose facilities.

Processors and generator manufacturers should already set their prices such that their costs are fully recovered, given their commercial nature. However, in cases where subsidies are provided by governments to certain processors or generator manufacturers, these should be removed to ensure that the move to sustainable economics can be achieved. For example, any government subsidies for the management or disposal of the wastes produced from the processing of ^{99}Mo irradiated targets should become the responsibility of the supply chain, following the notion of full-cost recovery and allowing for equal opportunities for all processors in the global supply chain.

Full-cost recovery should be implemented by all producers that supply the global market, otherwise there will be distortions that could jeopardise the long-term economic sustainability of the irradiation providers and thus jeopardise the long-term supply security of $^{99}Mo/^{99m}Tc$. In addition, it should be recognised by all consumers within the global market that the price increases expected by the application of full-cost recovery should flow through the supply chain and should be reflected in the costs of the final medical procedure, to be reimbursed appropriately by the health care system. As shown in the *Economic Study* (NEA, 2010), the final impact on end-users would be reasonably small; however, the increases are necessary to ensure reliable supply in the future.

The full-cost recovery methodology described in this document is not a price-setting mechanism; it defines the cost elements and allocation methods, but it does not dictate the value of those costs nor prices that would be charged by entities operating commercially. Given varying costs and ownership structures, and national competition laws, international pricing-setting regulation would be difficult or impossible to implement. Nor is price-setting necessarily desirable; a full-cost recovery methodology would still allow for downstream stakeholders to benefit from efficiency improvements that lower production costs through offering lower prices (where sustainable).

The price increases that would be expected by the application of full-cost recovery should flow through the supply chain and should be reflected in the costs of the final medical procedure, to be reimbursed appropriately by the health care systems. Table 1 below shows the expected price increases for economic sustainability throughout the supply chain for several different investment scenarios, based on the type of irradiation/processing facility (FDIR = fully dedicated isotope reactor; MP = multipurpose reactor; Proc = processing facility). Table 2 shows the impact of the price increases on the end user with full-cost recovery at the reactor level and a complete flow-through in the supply chain.

Table 1. Supply chain prices for economic sustainability, in EUR/six-day curie EOP*[a]

	Required price increase	From reactor	From processor	From generator	From radiopharmacy
Current situation pre-shortage	n/a	45	315	375	1 810
FDIR no Proc	355	400	670	730	2 165
MP 20% no Proc	100	145	415	475	1 910
MP 50% no Proc	310	355	625	685	2 120
FDIR + Proc[b]	355 R; 185 P	400	855	915	2 350
MP 20% + Proc	100 R; 185 P	145	600	660	2 095
MP 50% + Proc	310 R; 185 P	355	810	870	2 305

MP 20% – no capital costs +Proc	10 R; 185 P	55	510	570	2 005
MP 50% – no capital costs + Proc	95 R; 185 P	140	595	650	2 090

* As with all values presented in this report, these values are meant to be illustrative of the situation being described and should not be construed as being the absolute true value. EOP = end of processing.

a. For simplicity, only the levelised unit cost of ^{99}Mo values calculated using a 5% discount rate for reactors and 10% for processors, 20-year payback are presented.

b. "+Proc" indicates that a processing facility is also constructed and the relevant capital costs are passed through the supply chain.

Table 2. Impact of price increases at hospital level

	Irradiation value within final radiopharmaceutical price (EUR)	Irradiation value as % of reimbursement rate
Pre-shortage situation	0.26	0.11
Required for economic sustainability	0.33-2.39	0.14-0.97

The NEA has also developed an Excel workbook[6] that allows operators to implement the full-cost identification methodology described in Figure 1. The workbook incorporates all the formulas of the methodology so that the operator would only be required to insert the costs and variables specific to their facility and the model will produce the results of the levelised unit cost of ^{99}Mo production at the facility.

Implementation of the HLG-MR Policy Approach

The HLG-MR policy approach recommends a target of June 2014 for the implementation of full-cost recovery (as well as its other recommendations). This recognises that the supply chain will require some time to prepare to move to full-cost recovery, including the time to adjust contracts within the system. This time would also allow the health community to become informed of the changes and to examine reimbursement rates and the effect of full-cost recovery on the costs of ^{99m}Tc-based medical tests. The HLG-MR recognised that this transition period cannot be too long, as it could affect the ability of providers of ^{99}Mo irradiation services to stay in business, greatly affecting long-term supply security.

To ensure the effective implementation of full-cost recovery from irradiation sources and allow for transparency and trust within the supply chain, the NEA has agreed to undertake a periodic review of the supply chain (a project that is currently underway). This review would indicate who is, and who is not, implementing the HLG-MR policy approach. Other governments may undertake their own review of irradiation facilities in their jurisdictions, where there is potential for government subsidisation of ^{99}Mo irradiation services.

The NEA is working with all major stakeholders to assist in the implementation of the HLG-MR policy approach. For example, it is involved in efforts by the European Commission (EC) to promote greater communication and co-ordination among supply chain participants to minimise the probability of another supply crisis in the future. The EC has established a new body, the European Observatory, with a mandate to monitor the ^{99}Mo/^{99m}Tc supply chain and make recommendations to the EC on how to achieve reliable, long-term supply of these isotopes in Europe, while taking into account the global nature of the supply chain.

The European Observatory has four working groups, each of which deals with an important aspect of ^{99}Mo/^{99m}Tc supply:

- co-ordination of reactor/irradiator scheduling;
- application of full-cost recovery;

[6] Available at: http://oecd-nea.org/med-radio/guidance/

- HEU-LEU conversion; and,
- existing and new infrastructure for ^{99}Mo/^{99m}Tc supply.

The NEA is active in all four working groups either as an observer or lead.

Outage Reserve Capacity

In addition to the application of full-cost recovery, the HLG-MR policy approach noted that outage reserve capacity (ORC)[7] for ^{99}Mo production should be sourced and paid for by the supply chain (Principle 2 of the HLG-MR policy approach, see footnote 2 on p. 2). The provision of ORC is not an item included in the full-cost recovery methodology, as ORC could be considered a product that is offered separately from irradiation services. It is expected that the full-cost methodology described in the NEA guidance document should also be applied to identifying the costs associated with the provision of ORC within a reactor. The NEA is currently developing a guidance document on ORC for ^{99}Mo/^{99m}Tc supply chain participants, which will be publicly available in the near future.

3. HEU-LEU Conversion

To increase the understanding of the economic and supply chain impacts of converting to the use of LEU targets for ^{99}Mo production, the NEA developed a capacity model and an economic model of the supply chain, using data from individual facilities, to examine the global impact from conversion. Information for the impact assessment came from an expert working group (made up of major supply chain participants), which met for two workshops. This information was supplemented by interviews with individual supply chain participants by the NEA, and NEA's own knowledge of the supply chain.

Capacity modelling

The capacity modelling started with ^{99}Mo capacity and production reference data on all current and potential irradiators and processors (as of June 2012) and then applied the observed and expected impacts of LEU-target conversion on various elements affecting capacity. Since the model is time and facility specific, the degree of impact can vary from one facility to another, recognising that facilities can be affected differently.

The NEA modelled three impact scenarios on an "all-in" situation, as well as two "challenges" situations. The three impact scenarios applied high, low and very low impacts to the reference data of the three situations. Under the high (or low) impact scenario the NEA applied the highest (or lowest) expected facility-specific impact on production capacity. The very low impact scenario assumes that the economic returns from ^{99}Mo irradiation services improves significantly such that reactors, where possible, displace other irradiations in order to return ^{99}Mo irradiation capacity to pre-conversion levels. The impact scenarios were then applied to the three "situations":

- ***"All-in" situation:*** shows the expected impact from LEU-target conversion on all current and potential irradiators and processors according to the facility-specific time schedules of operation, conversion (if applicable) and shutdown.

[7] Outage reserve capacity is required to ensure a reliable supply chain by providing back-up irradiation and/or processing capacity that can be called upon in the event of an unexpected shutdown. A reduction in ORC increases the risk of supply shortages, particularly during any unplanned outage situation.

- ***Economic-challenges situation:*** starts from the "all-in" situation and assumes that the current, unsustainable economics of the supply chain continues, such that only projects that could be constructed and operated without commercial funding proceed.
- ***Technology-challenges situation:*** starts from the "all-in" situation and assumes that new technologies and new entrants face a higher risk in implementing their projects.

The capacity and production scenarios were then compared to the projected demand to determine if the impacts of LEU-target conversion affected ^{99}Mo supply reliability. To account for the need for ORC, three different demand forecast situations were evaluated: no ORC requirements; low ORC requirements, and high ORC requirements.

It was agreed by the expert working group that there were no incremental capacity impacts on generator manufacturers or further downstream. However, it was recognised that generator manufacturers face logistical challenges during the conversion process from keeping production of generators from HEU- and LEU-based ^{99}Mo separate until they receive health approvals.

Results: capacity impacts

For both current irradiation capacity and processing production, conversion to using LEU targets does not create new long-term supply shortages; shortages are already expected given the final shutdown of a number of existing facilities over the next decade. However, LEU conversion does intensify these shortages by reducing available capacity.

Under the "all-in" and technology-challenges situations, supply is sufficient over the time period to 2030 for both irradiator capacity and processor production. LEU-target conversion does reduce effective capacity and production, but not to levels that are of concern (i.e. below expected demand). However, there are two periods (2014 and 2017) where processor production under the technology-challenges situation is tight compared to demand with a high ORC requirement.

Of significant concern, though, are the results of the impact scenarios in the economic-challenges situation. For both irradiation capacity and processing production, supply is not sufficient to meet demand in the long term (Figure 2).

Figure 2. Current and select new processing production of ^{99}Mo vs. demand under the economic-challenges situation

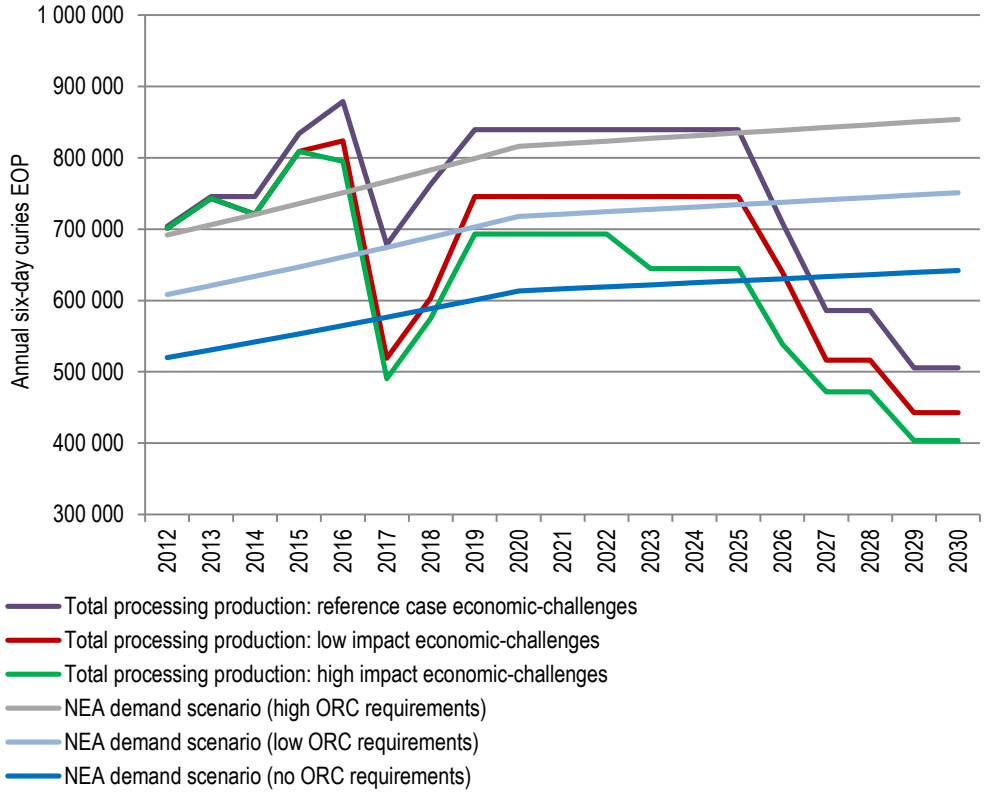

Under this scenario, LEU-target conversion accelerates the expected long-term shortages, creating a significant shortfall in 2017 resulting from one irradiator shutting down permanently. Between 2018 and 2025, LEU-target conversion keeps supply below the high-demand curve; by 2027 all scenarios (including the reference case) drop below the lowest demand curve.

The capacity impact modelling shows that, while LEU-target conversion does reduce available capacity and production, the main concern remains the unsustainable economics in the supply chain. In terms of capacity impacts, if the economic situation were to improve sufficiently to support adequate investment, LEU-target conversion should not create insecurity in ^{99}Mo supply.

Cost modelling

The cost modelling, as with the capacity modelling, started with a reference case for each currently operating ^{99}Mo irradiation or processing facility, as well as two new entrants: the FRM-II reactor in Germany and a reactor in Russia. Other new entrants were not modelled as they are planned as non-HEU production facilities.

The NEA modelled the impacts by applying high and low expected cost impact values to the reference case for individual facilities, based on the specific timelines of the facilities for operation, conversion and shutdown. The high and low expected values were coupled with the related capacity scenarios to undertake modelling using the levelised unit cost of ^{99}Mo (which takes into account changes in production). For example, high infrastructure cost values were applied to the low capacity impact scenario, as high upfront investment should minimise the capacity impact from conversion.

As with the capacity modelling, the expert working group determined that the main incremental cost impacts would be at the irradiator and processor stages of the supply chain. The cost impacts started at the uranium and target supply stages, which were modelled as processing

cost increases as processors are, in general, responsible for paying for targets. In this first stage, it was recognised that there would be an impact on the final cost of targets and on the research, development and qualification for these LEU targets.

For irradiators, the incremental cost impacts were related to the necessary infrastructure changes in the reactor. It was identified that either new irradiation rigs would be needed or they would have to be modified (to handle the different geometry of the new LEU targets), depending on the facility and the processor requirements. Cost impacts from reduced production (including required downtime) were calculated via the levelised unit cost of ^{99}Mo calculations, and other identified costs impacts (such as regulatory approvals) were included in processor conversion project costs, since irradiators indicated that they would pass the costs on to processors.

Processors face a number of incremental cost impacts, including costs from: modifying or developing new containers for transporting irradiated LEU targets (which also includes regulatory approval costs for the containers); infrastructure changes required to process changed targets and to increase waste storage; operating impacts; and supporting generator manufacturers in obtaining health regulatory approvals. Costs for these various cost impact elements vary across facilities and sometimes within the facilities themselves (in terms of high and low expected or observed impacts).

Results: cost impacts

Applying the range of expected facility- and time-specific cost impacts of the various impact elements to the facility reference case gives the expected results of the cost of converting to LEU targets for ^{99}Mo production. It should be noted that the reference case that is used for comparison is based on full-cost recovery of operations. The original capital costs are assumed to be fully amortised at the reactors and processing facilities that are converting and, thus are not included.

The following table shows the range of expected impacts from the various stages of the supply chain, when compared to the reference case of full-cost recovery. It is clear that LEU-based ^{99}Mo from a converted facility is more expensive than HEU-based ^{99}Mo from the same facility. The price increase, however, is less than 8% from the radiopharmacy, but is higher upstream.

Table 3. Range of cost increases for a 6-day curie of ^{99}Mo from the full-cost recovery reference case as a result of LEU-target conversion

	% increase in costs: range
From irradiator	3.6 - 36.8
From processor	6.3 - 42.8
From generator manufacturer	5.4 - 36.6
From radiopharmacy	1.1 - 7.8

The price increases translate to a reasonably small increase in relation to the reimbursement rate of the final diagnostic procedure. Based on a reimbursement rate of EUR 245 (a weighted average of global rates), the value of the radiopharmaceutical ^{99m}Tc increases from 4.46% of the reimbursement rate up to maximum of 4.8%. This translates to less than a EUR 1 increase[8] on a EUR 245 test. It should be noted, however, that even though the increase is small, it must still be funded, as it is important to support the upstream changes necessary. In a separate paper, the NEA discusses how unbundling the reimbursement for the isotope from the radiopharmaceutical

[8] It is important to note that these values are based on global averages; the values may vary between procedures and regions such that the isotope cost increases could be much higher for specific procedures or in certain regions.

and the diagnostic procedure could be a tool for greater transparency on necessary price changes[9].

Policy options to encourage LEU conversion

Current experience in the supply chain, unfortunately, seems to demonstrate that end payers have difficulty supporting even small changes in price. However, this support is necessary to ensure that the supply chain will have sufficient resources (and motivation) to convert to producing ^{99}Mo from LEU targets and to have sufficient capacity to ensure security of supply. In addition, the capacity study demonstrated that over the first few years of the conversion period, HEU-based ^{99}Mo will be available in sufficient quantities, and thus, with the price differences, it may be difficult to sell LEU-based ^{99}Mo. These two factors point to a need for governments to encourage non-HEU based ^{99}Mo production and consumer uptake, while respecting the HLG-MR policy approach to ensure a long-term secure supply of ^{99}Mo/^{99m}Tc (OECD/NEA, 2011).

The HLG-MR has developed a discussion paper that provides various options for governments to consider (OECD/NEA, 2012b)[10] to incentivise supply chain participants to convert to LEU-based targets. Broadly speaking, the policy options examined and described in that document have one of three roles:

- to make the option of purchasing or producing non-HEU-based ^{99}Mo and/or ^{99m}Tc more attractive, e.g. through reimbursement premiums for non-HEU production or funding for non-HEU ^{99}Mo/^{99m}Tc production capacity;
- to make the option of purchasing or producing HEU-based ^{99}Mo and/or ^{99m}Tc less attractive, e.g. through taxes on HEU-based production; or,
- limiting access to HEU-based ^{99}Mo/^{99m}Tc.

While countries may have differing views on the various options, given their own economic, regulatory, or political situation, this discussion paper provides a brief review of the options from the starting point of the HLG-MR policy approach to achieving a long-term reliable supply of ^{99}Mo/^{99m}Tc.

4. Conclusion

The implementation of the HGL-MR policy approach is essential to move forward towards a long-term secure supply of ^{99}Mo/^{99m}Tc. The approach takes into consideration the need for the supply chain to become economically sustainable in order to ensure the long-term security of supply. It is clear that any changes to the established way of producing ^{99}Mo/^{99m}Tc can create challenges for some supply chain participants and the results may not be exactly as expected. While the HLG-MR feels that its policy approach is the best direction for enacting necessary changes, finding the right balance and tools can take time. The provision for ongoing review as market changes occur should serve to monitor the market and adjust the policy approach as required.

Furthermore, it must be recognised that the commitment by the governments of all major ^{99}Mo/^{99m}Tc-producing countries to move towards LEU conversion, although for important non-proliferation reasons, creates an externality for the supply chain and increases production costs, without additional benefits to end users. These costs must be absorbed by all participants and reflected in the final reimbursement rate for ^{99m}Tc-based radiopharmaceuticals. In view of that, there is an important role for government to provide incentives to the supply chain to convert to LEU.

[9] http://oecd-nea.org/med-radio/discussion/docs/unbundling-payments.pdf

[10] Available at: http://oecd-nea.org/med-radio/discussion/docs/policy-options-ensuring-supply-security.pdf

5. References

Available at www.oecd-nea.org/med-radio:

OECD/NEA (2010), *The Supply of Medical Radioisotopes: An Economic Study of the Molybdenun-99 Supply Chain*, OECD, Paris, France.

OECD/NEA (2011), *The Supply of Medical Radioisotopes: The Path to Reliability*, OECD, Paris, France.

OECD/NEA (2012a), *Full-cost Recovery for Molybdenum-99 Irradiation Services: Methodology and Implementation*, OECD, Paris, France.

OECD/NEA (2012b), *The Supply of Medical Radioisotopes: Policy Options for Ensuring Long-term Supply Security of Molybdenum-99 and/or Technetium-99m Produced without Highly Enriched Uranium Targets*, OECD, Paris, France.

OECD/NEA (2012c), *The Supply of Medical Radioisotopes: Market Impacts of Converting to Low-enriched Uranium Targets for Medical Isotope*, OECD, Paris, France.

THYROID DOSES RECEIVED BY THE PUBLIC OF BELARUS DUE TO THE FUKUSHIMA-DAIICHI NUCLEAR ACCIDENT

J. KENIGSBERG
National Commission on Radiation Protection
Academicheskaya str., 8, 220012, Minsk – Republic of Belarus

K. KOUTS
Republican Scientific-Practical Center of Hygiene
Academicheskaya str., 8, 220012, Minsk – Republic of Belarus

ABSTRACT

Due to the accident at the «Fukushima-Daiichi», Belarus strengthened the monitoring of gamma-radiation dose rate and radionuclides concentration in the air. Assessment of thyroid doses received by the public in Belarus due to the inhaled iodine-131 has been implemented to respond to increased public concern regarding the impact of discharges to public health and to determine the appropriateness to take tablets of stable iodine. The main attention was paid to the age group «1-2 year old children» due to the fact that after the Chernobyl accident maximum thyroid doses were observed among children of this age. The assessment showed that thyroid doses to children varied from 5×10^{-7} mSv to 7×10^{-5} mSv. The observed thyroid doses are so insignificant that statistically they are not able to influence thyroid cancer morbidity among the Belarussian population.

1. Introduction

The magnitude 9.0 Great East Japan earthquake and the ensuing large tsunami (the inundation height around units 1 to 4 was between 11.5 m and 15.5 m above sea level), which occurred on the east coast of northern Japan on March 11, 2011, caused severe nuclear accident at the «Fukushima-Daiichi» nuclear power plant (NPP). This event has been rated at the highest level 7 on the IAEA International Nuclear Event Scale. Huge amount of radioactive materials, including iodine-131, cesium-134 and cesium-137, was emitted from the plant to the environment as the result of the nuclear accident. The hydrogen explosions in units 1 – 4 of the «Fukushima-Daiichi» NPP led to the worsening of the radiation situation. According to the different estimations [1, 2] about 1.6 – 2.0×10^{17} Bq of iodine-131, 2.8×10^{16} Bq of cesium-134 and 1.5 – 3.7×10^{16} Bq of cesium-137 were discharged to the atmosphere as the result of the accident. The activity of discharged radioisotopes is comparable with the activity released to the environment by the Chernobyl accident (1.8×10^{18} Bq of iodine-131, 4.7×10^{16} Bq of cesium-134 and 8.5×10^{16} Bq of cesium-137 [3]).

The accident at the Japanese NPP is a bright example of an accident with transboundary effect. Due to the influence of air masses the emissions of iodine-131 and radioisotopes of cesium were transferred over long distances, resulting in the contamination of the environment. Iodine-131 is a leading factor of internal exposure at the early stage of the accident. Thyroid gland exposure to radioiodine released from the Chernobyl accident has led to the unprecedented increase in thyroid cancer morbidity among the population of Belarus, Russian and Ukraine.

Assessment of thyroid doses received by the public in Belarus due to the inhaled «fukushima» iodine-131 has been implemented to respond to increased public concern regarding the impact of atmospheric discharges to public health and to determine the appropriateness to take tablets of stable iodine.

2. Material and methods

Due to the accident at the Fukushima-Daiichi many countries, including Belarus, have strengthened the monitoring of gamma-radiation dose rate, as well as the monitoring of radionuclides concentration in the air and in goods exported from Japan. According to the daily reports of World Health Organisation the radiation monitoring have been introduced in

the USA, Singapore, Australia, Malaysia, New Caledonia, Republic of Korea, the Philippines, Russia, China, on Taiwan and in the territory of the European Union.

After the accident slight amounts of iodine-131 were detected in the air of Belarus. The Republican Centre for Radiation Control and Environmental Monitoring (the RCRCEM) of the Hydrometeorology Department of the Ministry of Natural Resources and Environmental Protection of Belarus was carrying out the monitoring of iodine-131 activity concentration in the air. The RCRCEM is a centre which in the framework of the National System of Environmental Monitoring of Belarus monitors contamination of air, surface water, soils, precipitations and snow cover to assess anthropogenic impact on the mentioned environment components due to the discharges of pollutants and their transboundary transport.

The control of iodine-131 concentration in the air was being carried out at seven monitoring stations: Minsk, Mogilev, Mstislavl, Gomel, Mozyr, Pinsk and Braslav (fig1).

Fig.1 Location of monitoring stations to control activity concentration of iodine-131 in the air

According to the RCRCEM data at the moment of starting the monitoring (March 24, 2011) the activity concentration of iodine-131 in the air varied from 0.00004 to 0.0001 Bq/m^3. It reached its maximum about 24 days after the accident and was about:

- 0.004 Bq/m^3 in Minsk, Pinsk and Braslav,
- 0.005 Bq/m^3 in Mogilev and Mstislavl, and
- 0.001 Bq/m^3 in Mozyr.

Iodine-131 concentration in the air began to decline after April 3, 2011 and in a month after the accident was about 0.0001 Bq/m^3. Activity concentration levels detected on the Belarussian territory over the entire period of observations as well as their fluctuations were comparable with the levels recorded in the air of Kiev, Ukraine[1] (fig.2).

[1] On the basis of data of the Central Geophysical Observatory of Ukraine.

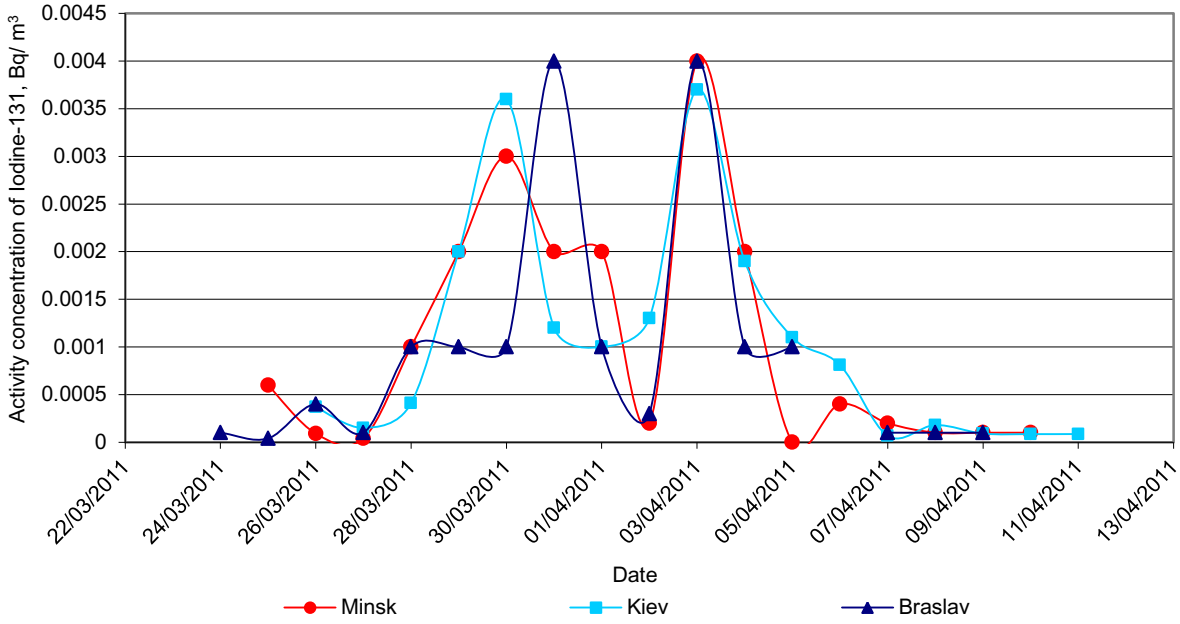

Fig. 2 Time variation of the activity concentration of iodine-131 in the air of Minsk, Braslav (Belarus) and Kiev (Ukraine)

The assessment was performed in compliance with the IAEA recommendations [4] on the basis of recoded data and taking into account the relevant dose coefficient for iodine-131[2]. The main attention was paid to the age group «1-2 year old children» due to the fact that after the Chernobyl accident maximum thyroid doses were observed among children of this age. The next formula was used to calculate the inhalation component of equivalent dose to the thyroid:

$$H_{thy} = X \times R_{inh} \times DF_{thy} \times t \,,$$

where

H_{thy} – equivalent dose to the thyroid due to the inhaled iodine-131, Sv;
X – activity concentration of iodine-131 in the air, (Bq/m^3);
R_{inh} – breathing rate (R_{inh} = 5.2 m^3/day for a 1-2 year old child);
DF_{thy} – equivalent dose to the thyroid per unit intake of iodine-131 via inhalation (DF_{thy} = 2.53 ×10^{-6} Sv/Bq);
t – time of exposure, day.

3. Results and discussion

Thyroid doses to the public of Belarus as the result of the accident at the «Fukushima-Daiichi» NPP were conditioned by the inhalation of radioactive iodine. Thyroid doses due to the ingestion of «fukushima» iodine-131 were considered as equal to zero because of the negligible low ground deposition of iodine-131 and absence of goods import from Japan.

Assessed thyroid doses received by the children due to the inhalation of radioiodine varied from 5×10^{-7} mSv to 7×10^{-5} mSv (fig.3) with the average thyroid dose observed over the period from March 28, 2011 to Apri 5, 2011 equal to 2.1×10^{-5} mSv. The maximum values were registered in 24 days after the accident in the Eastern part of Belarus, in Mogilev region.

[2] Dose coefficients are based on the compartment model of ICRP which describes the biokinetic of iodine in the body.

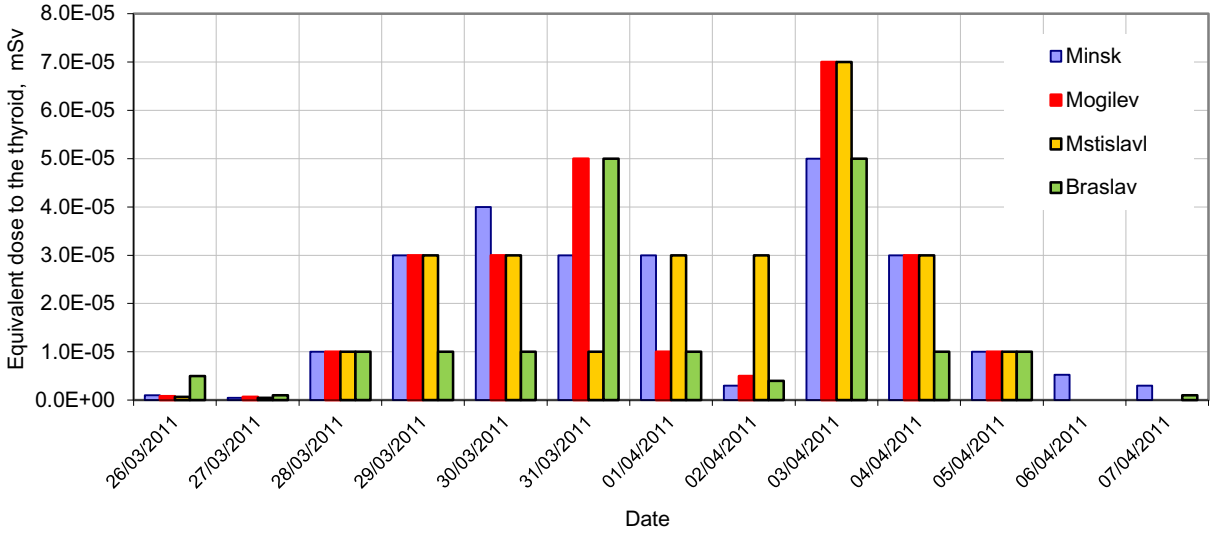

Fig 3. The evolution of thyroid doses received by the 1-2 year old children of Belarus

Low concentrations of iodine-131 in the air and, consequently, low thyroid doses are explained, first of all, by the distance from the Republic of Belarus to the scene of the accident (Belarus is situated 8 000 kilometers far away from the «Fukushima-Daiichi» NPP), and by the natural processes of radioactive decay (the half-life for iodine-131 is 8 days).

According to the latest requirements of the IAEA [5] the generic criteria (in terms of the dose that has been projected or the dose that has been received) for response actions to protect thyroid gland and to reduce the risk of stochastic effects (thyroid blocking) is 50 mSv. Therefore, taking into account daily measurements of iodine-131 activity concentration, thyroid doses received by «1-2 year old children» were million and more times less than the generic criteria.

4. Conclusion

The Republic of Belarus is situated 8 000 kilometers far away from the «Fukushima-Daiichi» NPP. So long distance from the source of emergency release, which is comparable with the activity released to the environment by the Chernobyl accident, caused that only slight amounts of iodine-131 have been detected in the air of Belarus. Nevertheless, the negative experience of response to the accident at Chernobyl NPP, which led to the increase in thyroid cancer morbidity among the population of three the most affected countries, caused the increase in public anxiety regarding the new radiation accident and, as the result, stimulated to the evaluation of thyroid doses to the public on the base of radiation monitoring of iodine radionuclides in the air. The assessment shown that observed thyroid doses were million and more times less than the IAEA generic criteria for protective actions and other response actions in emergency exposure situations to reduce the risk of stochastic effects.

Observed thyroid doses obtained as the result of the accident at «Fukushima-Daiichi» are so insignificant that did not require any protective actions and statistically are not able to influence thyroid cancer morbidity among the Belarussian population.

References

1. Report of Japanese Government to the IAEA Ministerial Conference on Nuclear Safety - The Accident at TEPCO's Fukushima Nuclear Power Stations // International Atomic Energy Agency [Electronic resource]. – 2012. – Mode of access: http://www.iaea.org/newscenter/focus/fukushima/japan-report/. – Date of access: 02.05.2012

2. Summary of the Fukushima accident's impact on the environment in Japan, one year after the accident // Institut de Radioprotection et de Sûreté Nucléaire [Electronic resource]. – 2012. – Mode of access: http://www.irsn.fr/EN/publications/thematic/fukushima/Documents/IRSN_Fukushima-Environment-consequences_28022012.pdf. – Date of access: 07.05.2012

3. Sources and effects of ionizing radiation. United Nations Scientific Committee on the Effects of Atomic Radiation : UNSCEAR 2008 Rep. to the General Assembly with scientific annexes : in 2 vol. / United Nations Scientific Committee on the Effects of Atomic Radiation. – New York : United Nations, 2011. – Vol. II, Annex D : Health effects due to radiation from the Chernobyl accident. – 173 p.

4. Generic procedures for assessment and response during a radiological emergency : IAEA-TECDOC-1162 / Intern. Atomic Energy Agency. – Vienna : IAEA, 2002. – 186 p.

5. Radiation Protection and Safety of Radiation Sources: International Basic Safety Standards. Interim Edition. GSG Part 3 / Intern. Atomic Energy Agency. – Vienna : IAEA, 2011. – 282 p.

MODELLING OF PARTICULATE CONTAMINANT TRANSFERS IN VENTILATED ROOMS - APPLICATION AND VALIDATION AT REACTOR BUILDING SCALE

H. Mohand-kaci[1,2], L. Ricciardi[1], S. Jahan[2], E. Gaillard-Lecanu[2], J. Fazileabasse[2], M. Lestang[3], L. Bouilloux[1], C. Prevost[1]

[1] Institut de Radioprotection et de Sûreté Nucléaire (IRSN), Saclay, France

[2] EDF R&D, STEP, Chatou, France

[3] EDF DPN UNIE, GPRE, St Denis, France

Abstract

Assessing the transfer of particles likely to be inhaled by an operator in a ventilated room is a major concern in many hazard industries, particularly in the nuclear sector. Predicting the distribution of a particulate contaminant is essential for risk management and the choice of collective and individual protection equipments; it can also help in optimizing the location and setting of monitoring devices.

For this purpose, a research program is being conducted for several years by EDF R&D and IRSN to develop and validate a multidimensional model for aerosol transfer in ventilated rooms. The model, implemented in the free EDF code *Code_Saturne* (Nérisson et al., 2011), is based on a simplified Eulerian approach. It is composed of a concentration transport equation taking into account various effects of particle deviation and migration, associated to an original model of wall boundary condition. This transport and deposition model was first validated on relatively simple geometries (sample ducts,...) and then on ventilated enclosures or rooms of different volumes (from 0.1 m^3 to 1500 m^3). The final step of this work is the validation at a reactor building scale (75,000 m^3), based on gaseous and particulate tracing experiments conducted during the outage of a 1300 MWe power reactor (PWR). First values of transfer coefficients estimated by the code at various measurement points throughout the building, following the injection of tracers at different source points, are overall in satisfactory agreement with experimental results, given the complexity of the geometry.

All the validations performed at various scales show the relevance of the developed model, which can be applied to any geometry (building, aerosol sampling line,...) and implemented in any open CFD code.

Keywords: Aerosol transfer, Particle deposition, Gas-particle flows, CFD simulations, Radiation protection

1 Introduction

Nowadays, people spend most of their time within confined atmospheres. However, pollution inside buildings or industrial rooms can have a great impact on the health of the occupants. Therefore, many studies have been published in recent years about a particulate contamination inside buildings and ventilated rooms (Lai and Nazaroff, 2000; Chen et al., 2006). Nevertheless, most authors are interested primarily in determining the overall rate of particle deposition in a ventilated room under different ventilation strategies, and few works attempt to accurately assess the amount of suspended contaminant likely to be inhaled by workers or detected by a measuring device.

Indoor particulate contamination is a significant concern in hazardous industry, as nuclear one. The control of the potential internal exposure of workers depends partly on the knowledge of the particulate contaminant concentration in the atmosphere of the RB, in particular at the workplaces. Hence an efficient prediction of the contaminant transfer inside a ventilated room can help in

optimizing the location and setting the radiation protection devices, which are essential for risk management and for collective protection equipment choice.

A research project involving IRSN and EDF was launched in order to introduce a validated aerosol transfer models allowing a relevant estimation of the aerosol transfer from a contamination point source to any potential location in the space. For that purpose, a phenomenological model was developed by Nérisson et al. (2011). The model has been implemented in a CFD code developed by EDF R&D, called Code_Saturne, and then validated for simple geometries (horizontal and vertical ducts, bends) and small ventilated rooms with various volumes (30 m^3 and 1500 m^3), by comparison to literature data and tracing experiments data. In order to make the aerosol transport and deposition model more general, additional deposition mechanisms such as thermophoresis and electrophoresis were implemented in the code and validated (Mohand-Kaci et al., 2010).

This aerosol transport and deposition model is built to be used for a wide range of geometries in industrial applications dealing with particulate contamination. For this purpose, a first validation in a PWR building (75,000 m^3) was carried out, based on aerosol and gaseous tracing experiments data during maintenance of a nuclear power plant. All these results are presented here.

In this study, airflow is considered as incompressible and is modelled using a RANS method (Reynolds Averaged Navier–Stokes). The turbulence is modelled with the standard $k-\varepsilon$ model.

It should be noted that for confidentiality reasons, the values of measured and calculated quantities will not be given in this paper.

2 Description of the aerosol model

Considering the size distribution of radioactive aerosols commonly encountered in nuclear facilities, the mass median aerodynamic diameter (MMAD) that has been considered is limited to a few tens of microns (less than 50 microns).

The relatively low inertia of such particles allows using a simplified Eulerian transport model, so called "Diffusion-Inertia model" (Zaichik et al., 2010). This model consists of only one transport equation of aerosol concentration, considering sedimentation, deviation from fluid streamlines and migration effects (Nérisson et al., 2011). The concentration transport equation of this model is written as follows:

$$\frac{\partial C}{\partial t}+\frac{\partial}{\partial x_i}\left\{\left[U_{f,i}+\tau_p g_i-\tau_p\left(\frac{\partial U_{f,i}}{\partial t}+U_{f,k}\frac{\partial U_{f,i}}{\partial x_k}\right)\right]C\right\} = \frac{\partial}{\partial x_i}\left[\left(D_B\delta_{ik}+D^t_{p,ik}\right)\frac{\partial C}{\partial x_k} + C\frac{\partial}{\partial x_k}\left(D_B\delta_{ik}+\frac{\Omega}{1+\Omega}D^t_{p,ik}\right)\right] \quad (1)$$

Where C: aerosol concentration (kg/m^3), U_f: fluid velocity (m/s), τ_p: relaxation time (s), g: gravity (m/s^2), D_B: Brownian diffusion coefficient (m^2/s), $D^t_{p,ik}$: particle turbulent dispersion tensor components (m^2/s), and Ω dimensionless turbulent Stokes number.

In the advection term at left side, the last two terms are respectively the sedimentation and the deviation of the particles relatively to the fluid streamlines. In the right hand side, the first term represents the turbulent and Brownian diffusions of particles, the second term represents the migration of particles due to thermophoresis effects (migration due to temperature gradient, negligible in the bulk flow) and turbophoresis effects (migration of particles from high-turbulence to low-turbulence regions). These latter effects are potentially important in jet flow.

A boundary layer approach has been developed by Nérisson et al. (2011) for aerosol flux prediction in the dynamic log-law wall region. For this purpose, Eq.(1) is rewritten in the near wall zone and then integrated in the dynamic log-law wall region, from the wall to a given point in the flow at a distance y normal to the wall (with $y^+ >> 1$), to obtain the following differential equation governing the concentration profile:

$$C\left(y^{+}\right)=\frac{J}{u^{*}V^{+}.\mathbf{n}}\left\{1-\exp\left[\frac{V^{+}.\mathbf{n}\sigma_{t}}{\kappa}\ln(y^{+})+V^{+}.\mathbf{n}\lambda(Sc_{B},\tau_{p}^{+})\right]\right\} \quad (2)$$

With J: particle flux to the wall, conventionally negative, y^+: dimensionless wall distance, **n**: vector normal to the wall, κ: Von Karman's constant, V^+: dimensionless velocity, u^*: fluid friction velocity (m/s) and σ_t : turbulent Schmidt number.

In Eq.(2), λ is a function based on semi-empirical formulas for each deposition regime. λ is depending on the dimensionless parameters Sc_B (Schmidt Brownian number) and τ_p^+ (dimensionless relaxation time of particles), such as :

$$\lambda(Sc_{B},\tau_{p}^{+})=\left[\frac{\tau_{p}^{+2n}}{\omega^{n}}+\left(\frac{Sc_{B}^{-\lambda_{1}}}{\lambda_{0}}\right)^{n}\right]^{-1/n} \quad (3)$$

In Eq.(3), ω, λ_0 and λ_1 are dimensionless parameters and equal respectively to 1700, 13.7 and 2/3, n = 2, $Sc_B=\nu_f/D_B$, ν_f : air viscosity $\left(m^2/s\right)$. This boundary condition approach at smooth walls determines the particle flux towards the wall in the boundary layer for any deposition regime and any surface orientation.

3 Methods

The ultimate goal of this work is to validate the aerosol transport and deposition model on a reactor building. This validation study is performed by comparing the experimental results obtained for gaseous and particulate transfers to results given by the numerical model.

3.1 Experimental method

The experiments were conducted by the IRSN Institute in a reactor building (RB), during its period of maintenance, in order to justify the relevance of the positions of radiation protection sampling devices. These experiments consisted in determining the gaseous transfer times, the gaseous transfer coefficients and the particles transfer coefficients. For this purpose, six gas release locations and two aerosol release locations were considered. The experiments consisted of continuous injection of tracers (gas and particles) at each release location and the tracer concentration was measured at all sampling locations. The gaseous and particles transfer coefficients were deduced from the concentration at equilibrium state. The sampling points for measuring tracer concentration were located at different levels in the RB (level -2 m up to level 32 m); air was sampled at six positions for each injection.

Two tracing techniques of polluants transfers were used in this experimental campaign:

- the first technique consisted in using the Sulfur Hexafluoride (SF_6) as a gaseous tracer to study the gases behaviour inside the building,
- the second technique consisted in using the particle tracer Fluorescein Sodium (uranine) to simulate the behaviour of mass median aerodynamic particulate diameters of 1.2 micron and 4.9 microns.

Experimental data collected during this measurement campaign were used as a reference for the validation of the aerosols transport and deposition model.

It should be noted that only the gas transfer times were measured experimentally because particulate tracers' concentration cannot be measured in real time and continuously. However, the particle transfer time is either identical or greater than the gas transfer time, mostly depending on the particles deposition rates.

3.2 Numerical method

To conduct efficient validation of the numerical model, a particular attention is required for the conformity of the CAD and for the generated mesh. In addition, precise knowledge of the input data is critical for a relevant comparison with experimental results. For this fact, an important preliminary work has been done concerning the validation of the reactor building geometry, study of the ventilation system, and the inlet and outlet flow rates. The ventilation system consists of two main networks. A first network that brings air into the building and extracts the same amount of air at the high dome, and a second network that provides air recirculation by extracting air at the dome and reintroducing it at the bottom level. The two networks are connected to a manifold where the air is then redirected to different building's rooms. The ventilation network consists of 31 inlets and 18 outlets conditions. In addition, parametric simulations were performed to examine the mesh sensitivity.

After the preliminary steps outlined above, the validation of model was performed in two stages. First, the gas tracer measurements (gaseous transfer coefficients and transfer times) were simulated to ensure the relevance of numerical airflows modelling. Then, the particle tracer tests were simulated to validate the particles drift and deposition terms in the model.

The total volume of the reactor building mesh is about 75,000 m^3. The mesh of the whole geometry is constituted of 30 million tetrahedral cells whose maximum side size is approximately 20 cm. The geometry of the RB and a mesh local view are given in Fig. 1.

Note that the thermal effects were neglected in all simulations. The temperature differences observed inside the BR during the experiments do not justify taking into account these effects.

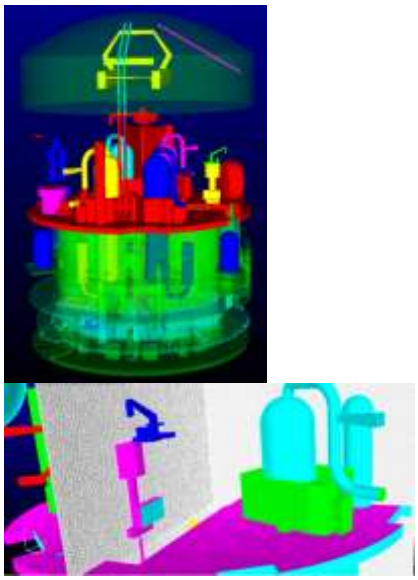

***Figure 1** : Reactor building geometry and adopted mesh*

4 Results

In this study, we first simulate the steady state airflow inside the building under experimental conditions. After that, we simulate the gas and particles transfer with solving of airflow disabled. The airflow streamlines (Fig. 2) show the dynamics of airflow inside the reactor building. The air is blown at lowest level and redirected to the annular space. The RB ventilation system provides the upward air flow movement from the lowest to the dome's top level where the air is extracted. The recirculation flow helps to ensure a good homogenization of airflow in the entire domain.

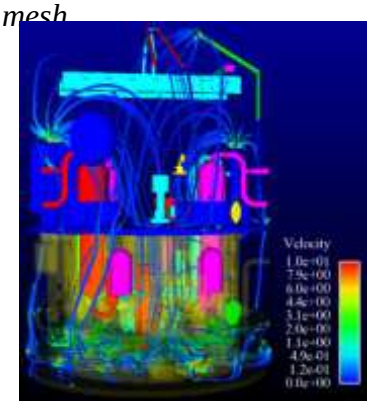

***Figure 2** : 3D streamlines in RB fluid domain*

4.1 Gaseous transfer coefficients

To validate the numerical simulation of air flow fields in the reactor building, we compared the gaseous transfer coefficients obtained experimentally to those estimated numerically. The transfer coefficient represents the ratio of gas concentration C^* (kg/m^3) measured at equilibrium state at one sampling point, to the gas injection mass flow rate q (kg/s):

$$k = \frac{C^*}{q} \tag{4}$$

In Fig. 3 we compare the numerical and experimental gaseous transfer coefficients associated to each of six release locations. The transfer coefficients presented below are averaged over all sampling locations and normalized by the experimental values. The results reported in Fig. 3 show a good agreement between numerical and experimental results, for all gas injections. The average deviation between numerical and experimental results is about 10 %. The maximum deviation reaches 17% (SG2 release location) and the minimum deviation is about 6% (RPS release location). Overall, the experimental and numerical results confirm the homogeneity of reactor building airflow in the main reactor zones, as the transfer coefficients results varies weakly. The numerical and experimental results agreement attests the relevance of the airflow simulation in the reactor building. The deviation observed can be attributed to the calculations assumptions and the simplifications performed on input data (geometry, flow rate values, ...).

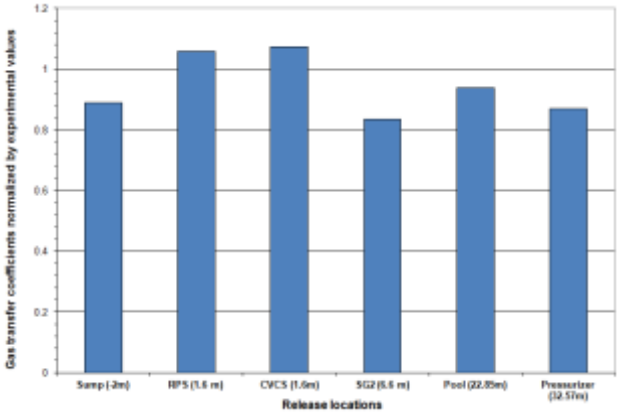

***Figure 3** : Mean gaseous transfer coefficients at each release location*

4.2 Gaseous transfer times

Gaseous transfer time inside the reactor building for various release locations is a very relevant validation way. For this purpose, the gaseous transfer times measured experimentally were compared to the numerical values for the six gas injection. The results, normalized by the experimental values, are averaged and plotted in Fig. 4. Overall, a good agreement is observed between simulation and experiment results. The mean transfer time is slightly overestimated for two release locations and weakly underestimated for one release location. These comparisons consolidate and validate the numerical simulations method.

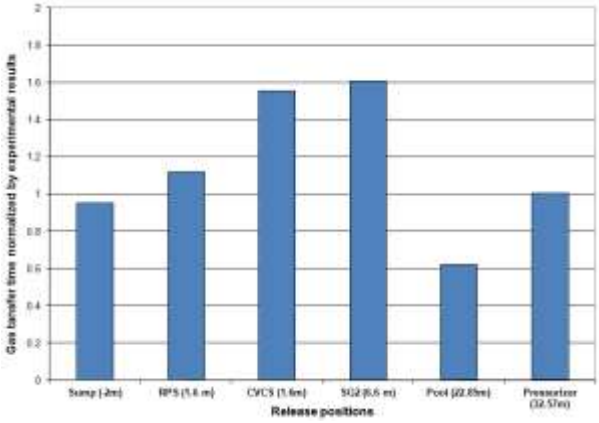

***Figure 4** : average gaseous transfer times*

4.3 Particles transfer coefficients

In order to validate the aerosol transport and deposition model presented in section 2, the particulate tracing experiments were simulated and the numerical results were compared to the experimental ones. Two release locations are considered: particles are injected at sump location (levels -2 m) and SG2 location (level 6.6 m). At each location, two particles size are considered: particles of uranine with mass median aerodynamic diameter (MMAD) of 1.2 µm and 4.9 µm with geometric standard deviation, σ_g , equal to 1.64 and 1.35 respectively. The particles are collected at six sampling locations as for gas injections. In the simulations, particle size distribution is divided into ten classes of particles. The particles transfer coefficients averaged values are shown in Fig. 5.

In the case of particles release performed at sump location, the transfer coefficients estimated numerically almost agree with the experimental results. In case of particles release performed at SG2 location, the numerical results agree with the experiments for particles of 1.2 µm diameter, but the results obtained for particles of 4.9 µm diameter are in less good agreement with experiments. Moreover, the airflow conditions when performing particle tracing experiments at SG2 were not fully known and controlled. This may partly explain the deviations observed between experiments and simulations results at SG2 point. Overall, Fig. 5 shows that the evolution of the transfer coefficients

predicted by the model is very consistent with the evolution of experimental measurements in both injection cases: transfer coefficients decrease as the particle size increases.

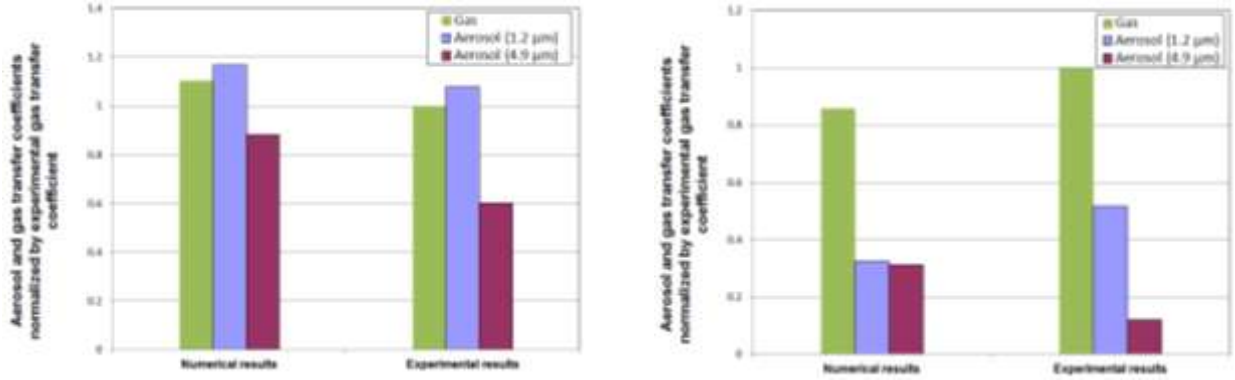

Aerosol release performed at sump (level -2 m) *Aerosol release performed at SG2 (level 6.6m)*

***Figure 5** : Particles transfer coefficients for two particle size distribution; MMAD = 1.2 µm and σ_g =1.64, MMAD=4.9 µm and σ_g =1.35*

The deviations between the numerical and experimental results can be attributed to the simplification performed in the geometry, which leads to reduce deposition surfaces and therefore to overestimate the concentration levels in the enclosure. This fact induces an overestimation of particle transfer coefficients. Due to the complexity of the geometry, these first results can be considered as satisfactory results. Nevertheless, additional experimental results are necessary to continue the validation process.

5 Conclusion

This paper discusses a first validation of a simplified aerosol transport and deposition model, introduced by Nérisson et al. (2011) and adapted at a very large scale. Previously, this model was validated for simple geometries and ventilated boxes of various volumes (30 m^3 and 1500 m^3). In this paper, a validation test, part of a validation process, was carried out in a very complex geometry: a reactor building. Comparison of simulation results to experimental measurements of gaseous and particulate tracers underlines the simulation ability to estimate correctly the air flows and contaminants transfer coefficients. Considering the complexity of the geometry and its important size, the results presented in this paper can be considered as satisfactory results. This study is a first validation of aerosol transfer model at industrial scale. To enhance the validation process, additional particulate and gas tracing experiments are planned in the reactor building. All these results will be presented in future.

6 References

Chen, F., Yu, S.C.M., Lai, A.C.K. (2006) *Modelling particle distribution and deposition in indoor environments with a new drift-flux model*, Atmospheric Environment **40**, 357-367.

Lai, A. C. K., Nazaroff, W. W. (2000) *Modelling indoor particle deposition from turbulent flow onto smooth surfaces*, Journal of Aerosol Science **31**, 463-476.

Mohand-Kaci, H., Ricciardi, L., Fazileabasse, J., Jahan, S., Douce, A. (2010) *Validation d'un modèle de transfert des aérosols à différentes échelles*, Congrès Français des Aérosols.

Nérisson, P., Simonin, O., Ricciardi, L., Douce, A., Fazileabasse, J. (2011) *Improved CFD transport and boundary conditions models for low-inertia particles*, Computers & Fluids **40**, 79–91.

Zaichik, L.I., Drobyshevsky, N.I., Filippov, A.S., Mukin, R.V., Strizhov, V.F. (2010) *A diffusion–inertia model for predicting dispersion and deposition of low-inertia particles in turbulent flows*, Int J Heat Mass Transfer **53**, 154–62.

Carbon ion irradiation suppresses metastasis related genes in human prostate carcinoma cells.

Annelies Suetens, Marjan Moreels, Kevin Tabury, Roel Quintens, Emiliano D'Agostino*, Sarah Baatout, Frank Deconinck.

*Radiobiology Unit and *Radiation protection, Dosimetry and Calibration Expert Group, Belgian Nuclear Research Centre, SCK•CEN, Boeretang 200, 2400 Mol, Belgium*

ABSTRACT

Hadrontherapy is a form of external radiation therapy, which uses beams of charged particles such as carbon ions. Compared to conventional X-ray therapy, the main advantage of hadrontherapy is the precise dose localization along with an increased biological effectiveness. This high ballistic accuracy allows depositing the maximal dose to the tumor, while damage to the surrounding healthy tissue is limited. First results obtained from prostate cancer patients treated with carbon ion therapy, show good local tumor control and survival rates. However, the impact of hadrontherapy on cancer metastasis is not yet well characterized. Previous studies have shown that hadrontherapy may inhibit metastasis by suppressing cell motility and migration. In contrast, clinical studies show evidence that X-rays might promote the metastatic potential of cancer cells. In the present study we investigated the effect of carbon and X-irradiation on changes in metastasis related genes in the human prostate adenocarcinoma cell line, PC3.

PC3 cells were irradiated with various doses (0, 0.5, 2 Gy) of accelerated ^{13}C-ions (75 MeV/u; LET = 33.4 keV/µm) at the GANIL facility (France). A similar experiment with X-rays (Pantak HF420 RX machine; 250 keV, 15 mA; dose rate= 0,25Gy/min) was performed at SCK•CEN (Belgium). RNA was extracted 8 h after irradiation. After labeling, samples were hybridized to Human Gene 1.0 ST Array chips (Affymetrix) and gene expression profiles were analyzed using Partek software. Our initial results demonstrate that carbon irradiation induced more strongly effects at the level of gene expression compared to similar doses of X-rays. For instance, within a set of genes related to cell motility and migration we found seven genes (APC, NEXN, MYH10, CCDC88A, ROCK1, FN1 and MYH9) with a significant fold change of <-3 after 2 Gy of carbon ion irradiation which were not as strongly affected by X-rays. A better understanding of the effects of different radiation qualities on the migration potential of prostate cancer cells is important for improving the clinical outcome of cancer radiation therapy.

1. Introduction

Prostate carcinoma is the second most frequently diagnosed cancer and the sixth leading cause of cancer death in males worldwide [1]. Radical prostatectomy, intensity modulated radiotherapy with X-rays and interstitial brachytherapy have been widely applied to treat clinically localized prostate cancer. Recent advances in radiotherapy, such as hadron therapy, have been included as a radiation treatment choice for prostate cancer. This type of external radiation therapy uses beams of accelerated charged particles, such as carbon ions, to hit the tumor [2]. Compared to conventional photon therapy, the main advantages of hadron therapy are the precise dose localization along with an increased biological effectiveness. This accounts for the highly lethal effects, even on radioresistant (with respect to X-rays) tumors. First results obtained from prostate cancer patients treated with carbon ion therapy, show good local tumor control and survival rates [3].

Although early stage prostate cancer can be treated very well, it can eventually progress to a more malignant cancer with highly invasive potential. Advanced prostate cancer often metastasizes to bone and lymph nodes and this is responsible for the majority of disease associated morbidity and mortality [4]. Metastasis is a multistep process that leads to the spread of cancer to distant organs [5]. In order to metastasize, cancer cells have to acquire

several properties, including migratory potential. A number of studies have identified differentially regulated genes that are expressed in the metastatic progression of prostate cancer [6]. The metastatic capability of cancer cells can be affected by many factors that influence cellular behavior. In this regard, therapeutic intervention might induce a metastatic phenotype. Both *in vitro* and *in vivo* data demonstrate that under certain circumstances photon irradiation promotes the metastatic potential of various types of cancer cells [7-10]. In contrast, it has been shown that carbon ion irradiation may inhibit metastasis by suppressing cell motility and migration *in vitro* [11-14]. To our knowledge the effects of different radiation qualities on gene expression of prostate cancer cells *in vitro* has not been verified so far.

In the present study we compared gene expression changes in the human prostate cancer cell line PC3 after irradiation with photon and carbon ion beams in order to elucidate radiation-specific biological effects. Differential gene expression through cDNA expression microarray was used to show the expression profiles of many genes including potentially important genes associated with cell migration. Our initial results demonstrate that carbon irradiation induced more strongly effects at the level of gene expression compared to similar doses of X-rays.

2. Materials and Methods

Cell culture. The human prostate adenocarcinoma cell line PC3 was obtained from the American Type Culture Collection (ATCC, Molsheim Cedex, France). This cell line exhibits highly invasive and metastatic activity and has been used for investigating biochemical changes in advanced prostate cancer [15]. PC3 cells were cultured in F-12K medium (ATCC) supplemented with 10% Fetal Bovine Serum (FBS) (GIBCO, Life Technologies, Ghent, Belgium) and maintained in a humidified incubator (37°C; 5% CO_2).

Irradiation. PC3 cells were irradiated with various doses (0, 0.5, 1 and 2 Gy) of accelerated ^{13}C-ions (75 MeV/u; LET = 33.4 keV/µm) at the Grand Accélérateur National d'Ions Lourds (GANIL) facility (Caen, France). Physical parameters of the beam can be found in table 1. A parallel experiment with X-rays (Pantak HF420 RX machine; 250 keV, 15 mA; average dose rate of 0,25Gy/min) was performed at the irradiation facility of SCK•CEN (Mol, Belgium). Control samples were treated in a similar matter, including transport, movement and positioning identical to, and simultaneous with, that of treated samples. For each condition 4 replicates were included.

Beam	$13C^{6+}$
Energy	75 MeV/u
Energy loss	about 4%
Calculated LET at the entrance of samples location	33.4 keV/µm
Flux	6.24×10^5 $cm^{-2}s^{-1}$
Spot size	around 4*4 mm^2

Table 1. Properties of the carbon ion beam in GANIL

Total RNA isolation and genome wide expression profiling. Samples irradiated with 0, 0.5 and 2 Gy were selected for further whole genome transcriptomic analysis using microarrays (8 h time-point). Total RNA was isolated according to the manufacturer's instructions using Qiagen kit (Qiagen, Venlo, The Netherlands). After labeling, samples were hybridized to Affymetrix Human Gene 1.0 ST Array chips (Affymetrix, Santa Clara, USA). Microarray analysis was performed using Partek Genomic Suite software (Partek Inc., St. Louis, USA). Three-way ANOVA analysis was done on gene level. ANOVA data were filtered based on gene sets found on Gene Ontology (GO) website.

Statistical analysis. The statistical significance of differences in gene expression between

control and each experimental condition for individual transcripts was determined using three-way ANOVA to generate raw p-values, while a False Discovery Rate (FDR) correction was used to correct for multiple testing. For general gene analysis and within the set of motility genes, only genes with a fold change (FC) of >2 or <-2 which had a FDR ≤ 0.05 were considered statistically significant. Within the set of motility genes, genes of interest were selected with a FC of < -3 (FDR < 0,05) induced by 2 Gy carbon ion irradiation.

3. Results

Gene expression profiles of PC3 cells were analyzed 8 h after exposure to different doses of carbon and X-irradiation. Microarray analysis followed by GO analysis allowed the identification of genes, as well as pathways which are enriched among statistically significant genes. We found that 2 Gy carbon ion irradiation affected the expression of 972 genes (733 downregulated and 239 upregulated) with at least 2-fold changes (FDR <0,05). Interestingly, after 2 Gy X-radiation only 60 genes were differentially expressed (45 downregulated and 15 upregulated), out of which 51 genes were common between both radiation types ($P = 1.35 \times 10^{-62}$) (Fig. 1A). To elucidate the involvement of specific biological processes in response to different radiation qualities, we assessed enrichment of certain GO categories among significant gene lists. Processes which were most significantly affected after 2 Gy of carbon ion irradiation included those associated with chromosome organization, cell cycle, microtubule-based processes and the DNA damage response (Fig. 1A). Genes that were affected by 2 Gy of X-rays were mainly involved in chromosome organization and DNA repair (Fig. 1A), indicating that the effect of ionizing radiation on microtubule-based processes (e.g. cell motility and migration) and the DNA damage response was specific for carbon ions.
Under these very strict conditions (FC >2; FDR <0,05) no genes were differentially expressed after exposure to 0.5 Gy of both radiation types, further confirming the radioresistant phenotype of these cells which may be explained in part by their p53 null status [16, 17].

Within the gene set related to cell motility (GO0048870), 34 genes changed at least 2 fold (FDR < 0.05) after 2 Gy carbon ion radiation (32 were downregulated, and 2 upregulated), while only 3 genes (all downregulated) were differentially expressed after 2 Gy X-irradiation (Fig. 1B). These 3 genes were common between both radiation types ($P < 10^{-12}$). As examples, we selected seven genes (APC, NEXN, MYH10, CCDC88A, ROCK1, FN1 and MYH9) that were most significantly downregulated (FC <-3, FDR <0.05) after 2 Gy of carbon ion irradiation. Examination of the magnitude of the changes in expression revealed that both carbon and X-irradiation induced a dose-dependent downregulation of these seven genes (Fig. 2). Interestingly, the impact of carbon irradiation on the expression level of these seven genes was more pronounced compared to similar doses of X-rays.

4. Discussion and conclusion

Carbon irradiation has gained in importance for prostate cancer treatment in part because of its improved dose localization and enhanced biological effect [3]. However, the many benefits of carbon ion radiotherapy need to be considered against the potential risks, including enhancement of metastasis and other potentially detrimental effects. The progression of cancer to metastasis depends on the dysregulation of signaling pathways, such as those associated with cell migration. Previous *in vitro* and *in vivo* studies demonstrated that after X-irradiation cancer cells might acquire a more aggressive phenotype, thereby favoring tumor recurrence and metastasis [7, 8, 10, 13, 18]. In contrast, *in vitro* studies showed that particle irradiation can have a suppressive effect on the migration of cancer cells [11-14]. So far, the

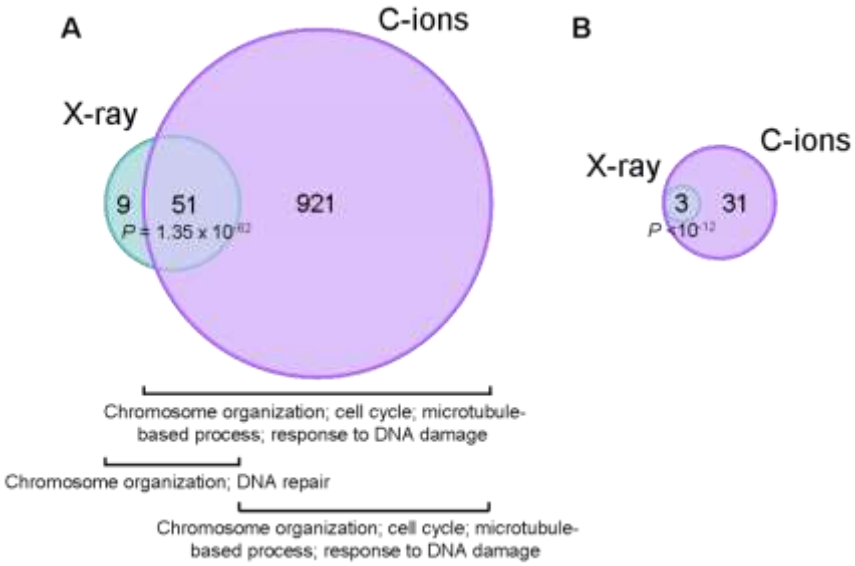

Figure 1: Magnitude of gene expression changes in X- and C-ion-irradiated PC3 cells. Venn diagrams summarize the overlap between both radiation qualities. *P*-values for the significance of the overlap are indicated. A: Overall changes in gene expression based on a -2< FC >2 and FDR <0.05. Enriched GO terms are shown below. B: Changes in gene expression based on a -2< FC >2 and FDR <0.05 among genes involved in cell motility.

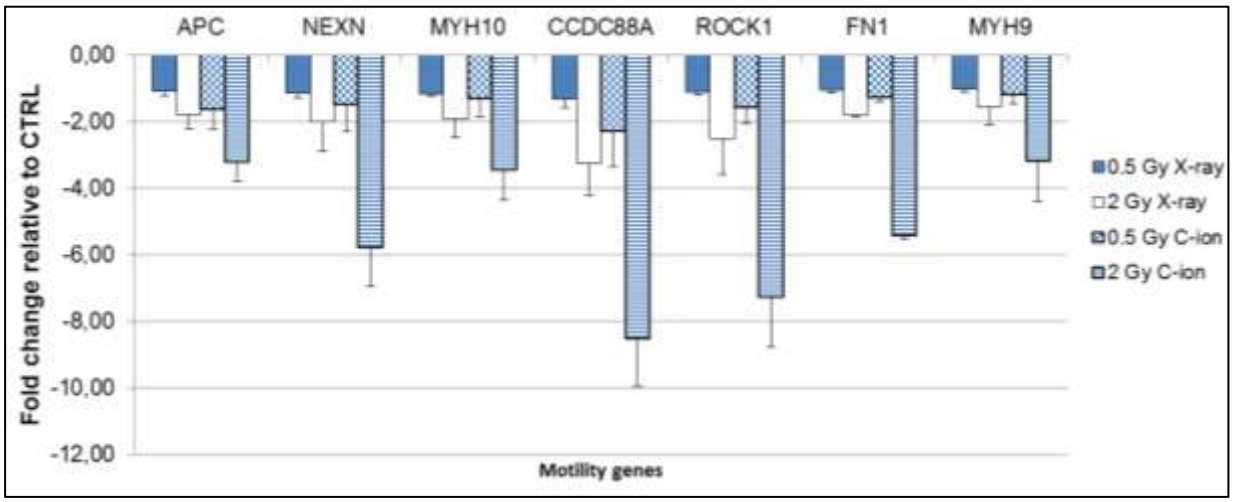

Figure 2: mRNA expression levels of radiation-responsive genes involved in cell motility (APC, NEXN, MYH10, CCDC88A, ROCK1, FN1 and MYH9). Both C-ion and X-irradiation induced a dose-dependent downregulation of the seven genes (fold change relative to non-irradiated CTRL).

underlying mechanisms of the observed differences between both radiation qualities are not completely understood. In the present study we compared the differences in transcriptional response to carbon and X-irradiation in the human prostate adenocarcinoma cell line, PC3.

First, we addressed whether carbon ions and X-irradiation differently affected global gene expression changes in PC3 cells. In general, our results demonstrate that carbon ion irradiation induced more pronounced expression changes in PC3 cells in terms of number of genes and magnitude of changes compared to X-rays. We found a strong overlap in gene expression changes between both radiation types indicating that similar processes are

affected. However, the biological effectiveness of 2 Gy carbon ion radiation at the level of gene expression is greatly increased compared to 2 Gy of X-rays. Our findings are in agreement with the study of Matsumoto et al. [19] who demonstrated that in melanoma cells the expression of many genes are more responsive to carbon ions compared to X-rays. However, our data show that carbon ions do have a specific effect on genes involved in microtubule-based processes (e.g. which are only mildly affected by X-irradiation).

Thus, our transcriptional analysis revealed a specific effect of carbon irradiation for instance on genes associated with cell motility and migration. The most significantly changed genes (APC, NEXN, MYH10, CCDC88A, ROCK1, FN1 and MYH9) had a fold change of <-3 after 2 Gy of carbon ion irradiation, which was much more attenuated after exposure to a similar dose of X-rays. These findings complement other recently published studies who demonstrated that carbon ion beams may induce a net suppressive effect on cell migration when compared to standard photon radiation [11-13]. Whether this stronger downregulating effect on motility related genes of carbon ion beams will also affect differences in cellular behavior (e.g. migration potential) is still under investigation. In addition, more research is needed to investigate whether these seven genes have a functional role in this prostate cancer cell line.

In conclusion, the main goal of this study was to analyze the biological effects of different types of radiation (carbon *vs*. X-rays) on the gene expression of prostate cancer cells. We found that under the conditions investigated carbon ion irradiation induced more pronounced changes in PC3 cells in terms of number of genes and magnitude of changes compared to X-rays. A better understanding of the effects of different radiation qualities on the migration potential of prostate cancer cells is important for improving the clinical outcome of cancer radiation therapy.

5. References

1. Jemal, A., et al., *Global cancer statistics.* CA Cancer J Clin, 2011. 61(2): p. 69-90.
2. Hamada, N., et al., *Recent advances in the biology of heavy-ion cancer therapy.* J Radiat Res, 2010. 51(4): p. 365-83.
3. Ishikawa, H., et al., *Carbon-ion radiation therapy for prostate cancer.* Int J Urol, 2012. 19(4): p. 296-305.
4. Koeneman, K.S., F. Yeung, and L.W. Chung, *Osteomimetic properties of prostate cancer cells: a hypothesis supporting the predilection of prostate cancer metastasis and growth in the bone environment.* Prostate, 1999. 39(4): p. 246-61.
5. Chambers, A.F., *The metastatic process: basic research and clinical implications.* Oncol Res, 1999. 11(4): p. 161-8.
6. Dasgupta, S., S. Srinidhi, and J.K. Vishwanatha, *Oncogenic activation in prostate cancer progression and metastasis: Molecular insights and future challenges.* J Carcinog, 2012. 11: p. 4.
7. Wild-Bode, C., et al., *Sublethal irradiation promotes migration and invasiveness of glioma cells: implications for radiotherapy of human glioblastoma.* Cancer Res, 2001. 61(6): p. 2744-50.
8. Pickhard, A.C., et al., *Inhibition of radiation induced migration of human head and neck squamous cell carcinoma cells by blocking of EGF receptor pathways.* BMC Cancer, 2011. 11: p. 388.
9. De Bacco, F., et al., *Induction of MET by ionizing radiation and its role in radioresistance and invasive growth of cancer.* J Natl Cancer Inst, 2011. 103(8): p. 645-61.
10. Fujita, M., et al., *X-ray irradiation and Rho-kinase inhibitor additively induce invasiveness of the cells of the pancreatic cancer line, MIAPaCa-2, which exhibits mesenchymal and amoeboid motility.* Cancer Sci, 2011. 102(4): p. 792-8.
11. Ogata, T., et al., *Particle irradiation suppresses metastatic potential of cancer cells.* Cancer Res, 2005. 65(1): p. 113-20.
12. Goetze, K., et al., *The impact of conventional and heavy ion irradiation on tumor cell migration in vitro.* Int J Radiat Biol, 2007. 83(11-12): p. 889-96.
13. Akino, Y., et al., *Carbon-ion beam irradiation effectively suppresses migration and invasion of human non-small-cell lung cancer cells.* Int J Radiat Oncol Biol Phys, 2009. 75(2): p. 475-81.

14. Fujita, M., et al., *Carbon-ion radiation enhances migration ability and invasiveness of the pancreatic cancer cell, PANC-1, in vitro.* Cancer Sci, 2012. 103(4): p. 677-83.
15. Kaighn, M.E., et al., *Establishment and characterization of a human prostatic carcinoma cell line (PC-3).* Invest Urol, 1979. 17(1): p. 16-23.
16. An, J., et al., *Overcoming the radioresistance of prostate cancer cells with a novel Bcl-2 inhibitor.* Oncogene, 2007. 26(5): p. 652-61.
17. Skvortsova, I., et al., *Intracellular signaling pathways regulating radioresistance of human prostate carcinoma cells.* Proteomics, 2008. 8(21): p. 4521-33.
18. Zhou, Y.C., et al., *Ionizing radiation promotes migration and invasion of cancer cells through transforming growth factor-beta-mediated epithelial-mesenchymal transition.* Int J Radiat Oncol Biol Phys, 2011. 81(5): p. 1530-7.
19. Matsumoto, Y., et al., *Gene expression analysis in human malignant melanoma cell lines exposed to carbon beams.* Int J Radiat Biol, 2008. 84(4): p. 299-314.

6. Acknowledgements

This work is partly supported by the ESA/ BELSPO MOSAIC2 contract (42-000-90-380) as well as by the Belgian Cancer Plan, Belgian Ministry of Public Health (CO-90-2088-01).

RESEARCH REACTOR CONTRIBUTIONS TO RENEWABLE ENERGY SOLUTIONS

E. VAN WALLE, H. BLOWFIELD, S. VAN DYCK
SCK•CEN
Boeretang, 2400 Mol - Belgium

ABSTRACT

Pure Silicon ingots can be loaded in research reactors where neutron irradiation allows the transformation of Silicon atoms into Phosphorus in order to obtain a semi-conductor material, called Neutron Transmutation Doped Silicon. The advantage of this technique is the high degree of homogeneity of Phosphorous doping and the consequent excellent uniform resistivity of the semi-conductor. The Belgian Reactor BR2 has several qualified devices that provide capacity to irradiate ingots up to 8" in diameter and this makes SCK•CEN a worldwide major producer of NTD-Silicon that is being used in high-tech applications that mainly serve renewable energy solutions.

1. Introduction

Silicon is, with the sole exception of oxygen, the most abundant element in the Earth's crust.. As we all know, pure Silicon is an intrinsic semiconductor that has a very high resistance to conducting electricity at normal room temperatures due to the non-presence of free electrons in the material. However, by 'adding' or 'creating' other elements within pure Silicon we can create a semi-conductor material that finds its application in the electronic industry. Here the element to be added is phosphorus: it can be added in a chemical way or it can be created by neutronic interaction on Silicon in a research reactor. The advantage of the latter technique is the high degree of homogeneity of Phosphorous doping and the consequent excellent uniform resistivity of the semi-conductor.

The Belgian Reactor BR2 is one of the worldwide major producers of neutron-transmuted-doped (NTD) Silicon with excellent irradiation capabilities and different devices that provide capacity to irradiate ingots up to 8" in diameter. This presentation will outline the present status of the BR2 activities on NTD Silicon and its applications that support renewable energy and other power related uses.

2. Doping methodologies of Silicon

In general we distinguish two methods: a chemical technique and a nuclear methodology.

The chemical gas doping method is based on the diffusion of Phosphorous that is added in different ways during the growth of a Silicon crystal: here temperature, Phosphorus flow and gas pressure are important parameters to obtain a doped crystal. The advantage of this technique is that it has a rather low cost and the process remains entirely within the control of the producer.

The nuclear method relies on a neutronic interaction with Silicon-nuclei that make up the Silicon crystal

$$30Si(n,\gamma)31Si \rightarrow 31P\ (stable\ element)$$

The result is stable Phosphorous atoms which give the silicon the electronic characteristics required for semiconductor applications and it is the result of this process that is referred to as N(eutron)T(ransmutation)D(oped) Silicon. The 'dis'advantage of this method is that you need a materials testing reactor, which makes it obviously more expensive to produce than the first chemical method.

However, the advantage of the nuclear method is that it produces a very uniformly doped Silicon crystal; more uniform than can be obtained with chemical methods. The consequence is that NTD Silicon is being used for 'high' power micro-electronic applications, whereas the chemically-doped Silicon is limited to 'low' power applications. Figure 1 shows the difference in uniformity.

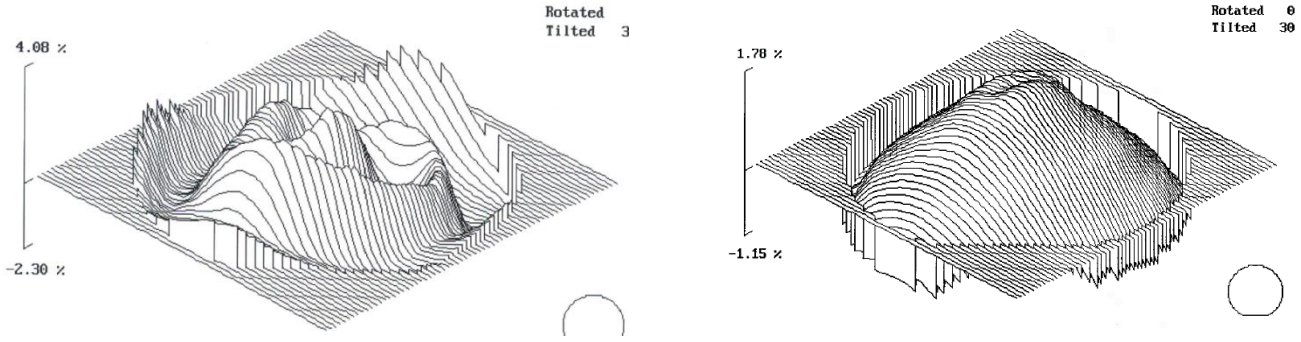

'best quality' in-situ doped 'good quality' NTD doped

Fig 1. Quality of doped Silicon (courtesy of TOPSIL)

3. Research reactor production of NTD-Silicon in BR2

There are several materials research reactors in the World that can produce NTD-Silicon. It is obvious that the degree of doping that determines the semiconductor resistivity of the Si-crystal, depends on the irradiation time and the neutron flux that is provided to the crystal. A low resistivity requires long irradiation times and high resistivity usually requires less. The homogeneity of irradiation depends on the reactor (neutron spectrum, neutron density) or, better, on the (geometrical) configuration in which the Silicon ingots are irradiated. A typical silicon ingot is shown in figure 2. The different research reactors in the World that have a considerable NTD-Silicon production are shown in figure 3. At SCK•CEN in Mol Belgium we produce NTD-Silicon in the Belgian Reactor 2 (BR2) Materials Testing Reactor.

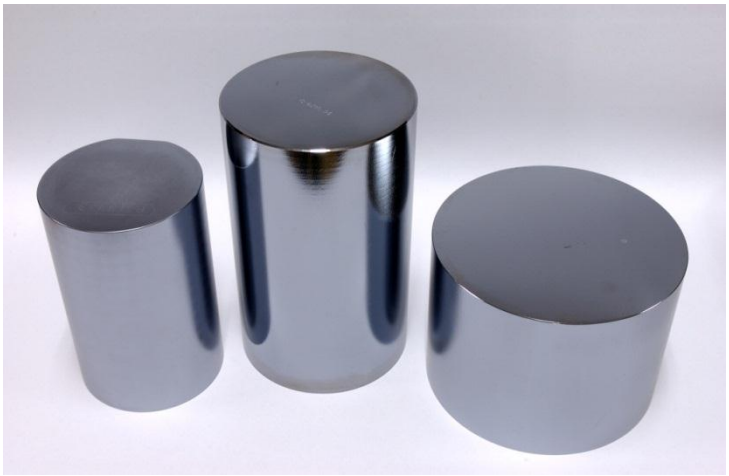

Fig 2. Silicon single crystal ingots

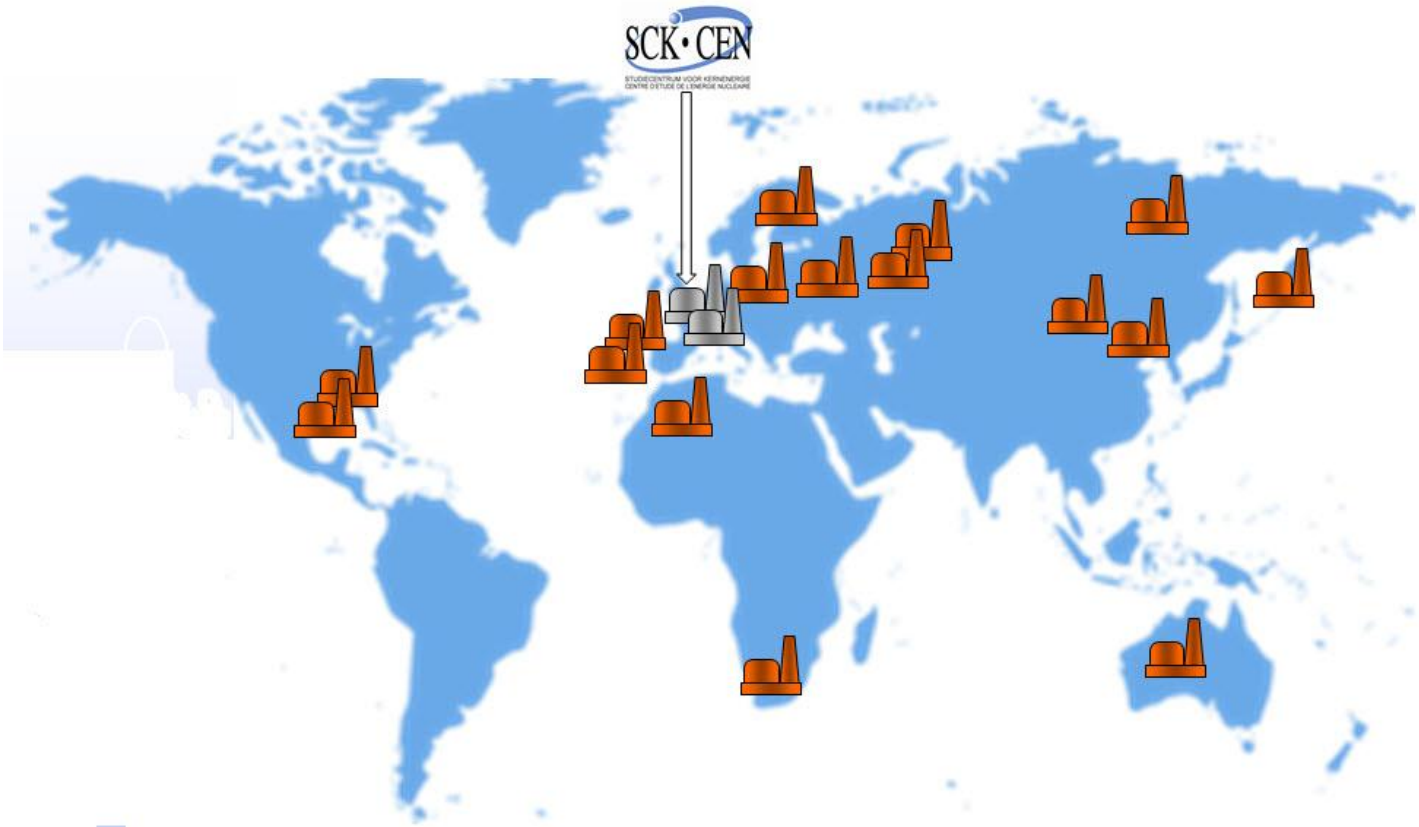

Fig 3. Research reactors in the world that produce NTD-Silicon

3.1 The BR2-reactor: a multi-disciplinary tool

The BR2 reactor is a high performance material test reactor. The reactor core is constructed as a number of cylindrical irradiation channels, arranged in a hyperboloid of revolution. This geometry is shown in figure 4 and allows a high core density on one hand, while maintaining good accessibility on the other hand: the diameter of the reactor vessel at the top and bottom covers is about double the diameter at the core level. Each irradiation channel is materialized in a beryllium block with hexagonal cross section. This beryllium serves as moderator, together with the light water in the channels, which acts as coolant. Inside each irradiation channel, fuel elements, control rods and experiments can be loaded in a flexible way as to satisfy the required irradiation conditions for all experiments.

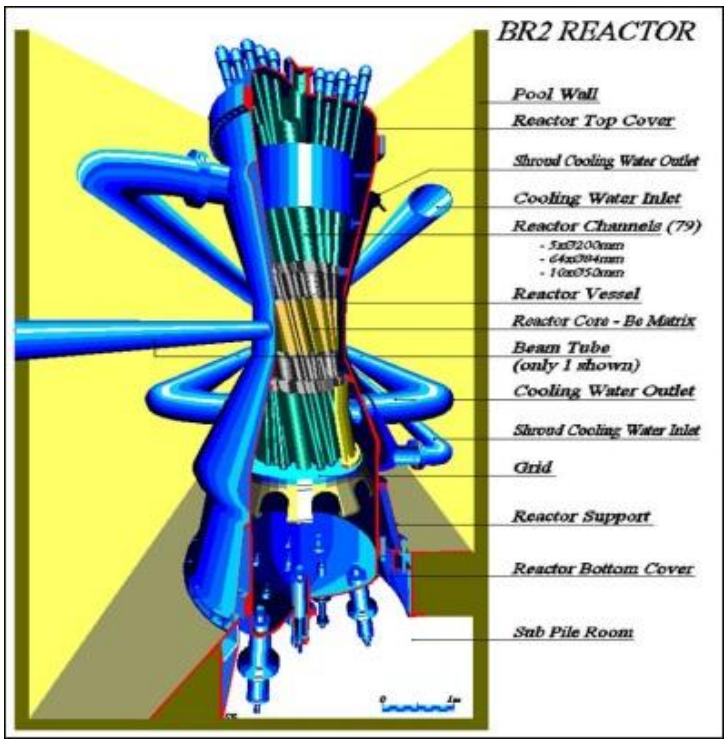

Fig 4. Geometry of the BR2 reactor

Due to the compactness of the reactor, a high flux density is obtained in the center of the core (up to 1015n/cm²s), while flux levels in the periphery of the reactor core drop down to a factor 10 lower.

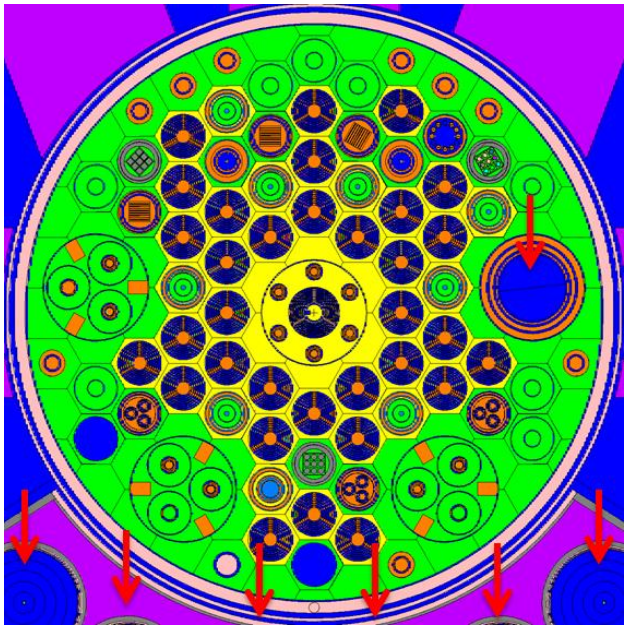

The operation of the reactor and the associated experiments is supported by 3 dimensional neutron transport modelling in order to predict the irradiation conditions in any point in the reactor as a function of the reactor operation cycles (figure 5). This model, using a Monte-Carlo method, coupled to a fuel burn-up code, is supported by on-line monitoring devices of the power and neutron flux in experimental devices.

Fig 5. Representation of a typical BR2 core load in the MCNP model of the reactor (mid plane). The position of NTD-Silicon irradiation devices is arrowed in red.

3.2 Silicon production in BR2: SIDONIE and POSEIDON

Description of the SIDONIE facility

SIDONIE (SIlicon DOping by Neutron Irradiation Experiment) is a single channel light-water device that is located in a 200-mm diameter beryllium channel (H2) within BR2's Reactor Pressure Vessel (RPV). It is designed to irradiate 5-inch diameter batches of silicon by continuously rotating and traversing them through the reactor neutron flux at predetermined, computer controlled speeds. This provides an exceptionally uniform exposure to neutrons *(see figure 6)* whilst controlling the neutron dose, and thereby producing the desired electronic characteristics within very precise limits. The baskets used to accommodate the silicon during irradiation are manufactured from aluminium and are of an "open" design. Accordingly, the silicon is in contact with the reactor pool water which under forced convection serves to maintain the surface temperature of the silicon considerably below 100 °C throughout the entire process. This water is highly purified and it is continuously monitored for contaminants, temperature and coolant flow.

Fig 6. SIDONIE facility

The SIDONIE facility is characterized by:

- a perturbed integrated 'conventional thermal flux' of approximately 2.8·1013 n·cm-2·s-1 as measured within the axis of specially prepared silicon crystals; to produce a typical target resistivity of 35 Ω·cm, starting of a resistivity of about 2000 Ω·cm (for N-type), requires a thermal neutron dose of approximately 7.43 x 1017 n·cm-2; this is achieved by an irradiation time of approximately 3.6 hours when operating at a normal reactor power of 55 MWth
- a cadmium ratio of approximately 25:1
- silicon irradiation-batch diameter of 5-inches (maximum)
- silicon crystal lengths of 300-mm (maximum)
- silicon irradiation-batch length 800-mm (maximum)
- a silicon core temperature of <200 oC during irradiation
- an NTD-silicon production capacity of approximately 15-tonnes per year based on 119-days (over 5 cycles) of reactor operation and an average target resistivity of 35 Ω·cm.

SIDONIE's NTD-silicon irradiation performance is characterised by:

- a deviation from target resistivities of typically <+/-5%
- Axial Resistivity Gradients (ARG) over 800-mm of <3% (for N-type silicon)
- Radial Resistivity Gradients (RRG) for 5-inch dia. of <3%
- an NTD-Silicon target resistivity production range from 5 to 500 Ω·cm

3.3 Description of the POSEIDON facility

POSEIDON (POol Side Equipment for Irradiation and DOping of silicon by Neutrons) is a multi-channel, graphite moderated device that is located in the BR2 reactor pool on the outside of the RPV *(see figure 7)*. It has the capability to simultaneously expose 6-batches of 6 and 8-inch diameter silicon to a highly homogenised 'conventional thermal flux' in a relatively low (about 26°C) temperature environment.

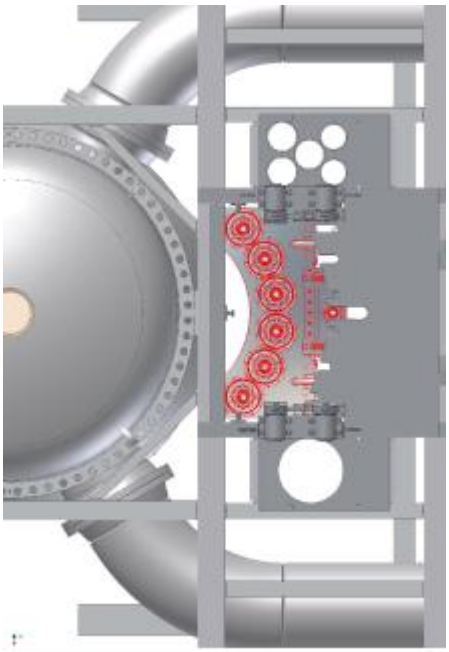

POSEIDON basically consists of a robust aluminium box of all welded construction to provide a sealed containment for high-purity graphite. This serves as an economical medium for preserving the 'conventional thermal flux' that would otherwise be totally lost from the reactor core through unavoidable leakage into the reactor pool. The external dimensions of the box are approximately 1.4 x 1 x 0.75 metre (WxHxL). However, one side of the box has been manufactured to conform to the radial profile of the RPV shroud whilst its height of 1 metre approximately spans the distance between the top and bottom of the reactor core. The box is penetrated by 6 vertical irradiation channels (through-holes) that form a concentric array around the curved profile of the box. This geometry enables the box to be brought into very close proximity to the RPV shroud so that each channel is of equal distance from the reactor core. During irradiation, the box is presented to the reactor so that the silicon is exposed to the optimum 'conventional thermal flux'.

Fig 7. Plan-view of POSEIDON at load/unload position

The irradiation is terminated by withdrawing the box a short distance away from the reactor and hence the neutron flux. This also provides the operational access required for charging and discharging the silicon from POSEIDON. POSEIDONs irradiation containers *(see figure 8)* are manufactured from aluminium and are designed to accommodate 500-mm long 'batches' of 8-inch diameter silicon consisting of 2 crystals approximately equal in length (250-mm + 250-mm) in a one-on-one arrangement. Using the same 'two-crystal' configuration, 'batches' of 6-inch diameter silicon are located in the same irradiation containers using graphite adaptor sleeves. These reduce the 8-inch bore of the containers to accept 6-inch diameter silicon without unduly compromising the intensity of the 'conventional thermal' flux that is available for irradiating the silicon. A uniform neutron exposure is obtained by continuously rotating the silicon throughout its irradiation and by replacing the top crystal with the one from beneath it and the bottom crystal with the one from above it at midpoint during the irradiation.

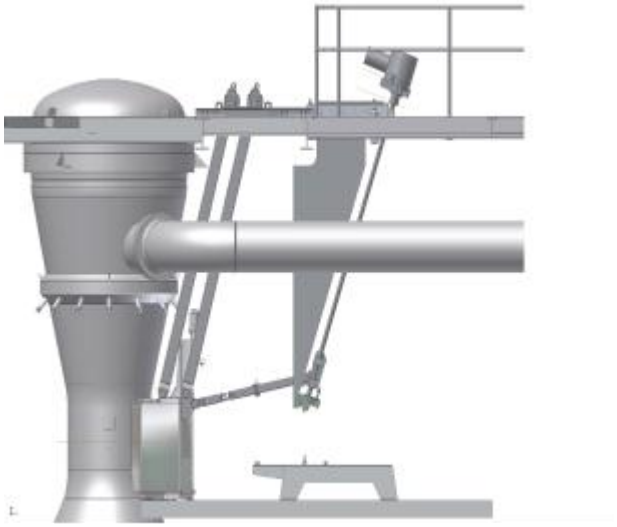

Fig 8. Side view of POSEIDON

Throughout irradiation, the silicon crystals come into direct contact with the reactor pool water which under natural convection serves to keep the surface temperature of the silicon considerably below 100^{o}C.

The POSEIDON facility is characterized by:

- a perturbed integrated 'conventional thermal flux' of about 5.26·1012 n·cm-2·s-1; for a typical target resistivity of 48 Ω·cm, starting from of a resistivity of about 2000 Ω·cm (N-type), the irradiation time is approximately 30 hours
- a cadmium ratio >50:1
- silicon irradiation-batch diameters of 6 and 8-inches
- silicon crystal lengths of 250-mm +/5-mm
- silicon irradiation-batch length 500-mm (maximum)
- a silicon core temperature of<200 oC during irradiation
- an NTD-silicon production capacity of approximately 18-tonnes per year based on 119-days (over 5 cycles) of reactor operation and an average target resistivity of 48 Ω·cm

POSEIDON's NTD-silicon irradiation performance is characterised by:

- a deviation from target resistivities of typically <+/-5%
- Axial Resistivity Gradients (ARG) over 500-mm of <+/-3% (for N-type silicon)
- Radial Resistivity Gradients (RRG) for 6-inch dia. of <4%
- an NTD-Silicon resistivity production range from 20 to 500 Ω·cm

3.4 BR1, a promising tool for high resistivity NTD-Silicon

The Belgian Reactor 1, or BR1, see Figure 9, was the first Belgian research reactor to become critical in 1956. BR1 uses natural uranium as fuel and the reactor consists of a stack of graphite blocks that act as a moderator. The reactor is air-cooled. The reactor has many access channels up to a diameter of 250mm and a useful internal length of 4 meters. The neutron field is very well characterised, well thermalised but is much lower than in BR2. These properties of BR1 make it however a very useful tool to produce high resistivity (> 400 Ωcm) NTD-Silicon, that requires less neutrons to obtain the final goal. A 'collection' of different diameters of Silicon ingots can be stacked in order to fill the channels and a 'feedthru' system is designed to easily load and unload the Silicon ingots. SCK•CEN envisages to increase the power of BR1 to increase the production capacity of the BR1-channels.

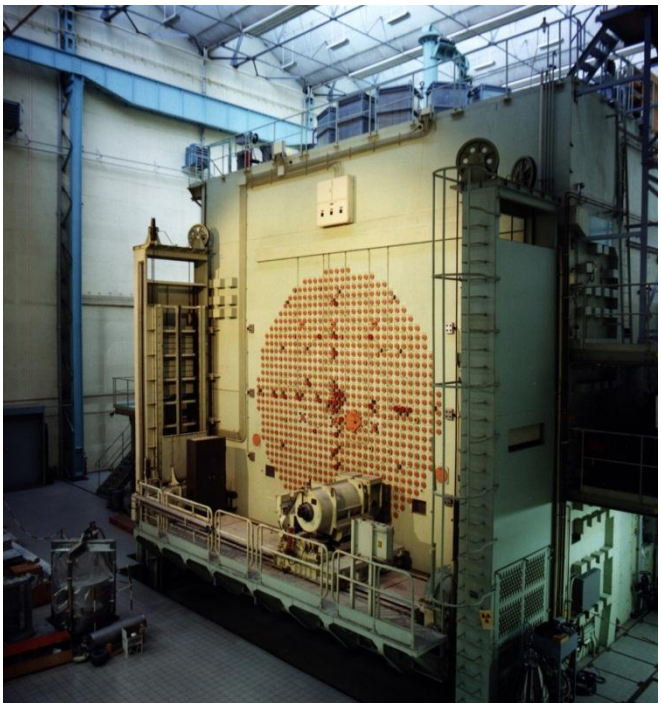

Fig 9. The BR1 reactor having large access channels for NTD-Silicon

Preliminary qualification tests have demonstrated capability to produce very good quality NTD-Silicon. The very well thermalised neutron spectrum also reduces the radiation damage that occurs due to irradiation.

We expect that the demand for high-resistivity semi-conductor material will increase substantially with the increasing demand for high-power applications from the renewable energy systems and their offsprings.

3.5 The future

The limited number of research reactors that are being used for NTD-Silicon production reach a typical age of 50 years. It is clear that Europe and the World will need to invest in new research reactors in order to safeguard the production of a number of applications. Besides NTD-Silicon there also the important issue of medical radio-isotopes. Within Europe a tripartite agreement has been reached between CEA (France), NRG (The Netherlands) and SCK•CEN (Belgium) that tries to assure the availability of future (research) reactor irradiation capacity in Europe. The agreement stipulates that these organisations push the idea in Europe to replace their existing research irradiation facilities (OSIRIS, HFR and BR2) by new research infrastructures: RJH (France), PALLAS (The Netherlands) and MYRRHA (Belgium) that can assure the material's research activities, the medical radio-isotope production and the NTD-Silicon production up to 2050. More information on the MYRRHA system can be found on the website of SCK•CEN under http://myrrha.sckcen.be/.

4. Applications of NTD-Silicon

The applications of NTD-Silicon are very versatile and the number has been growing steadily especially with the increase and evolution of renewable energy systems: more energy production per unit lies at the basis of the NTD-developments. As the power electronics of the renewable devices becomes more demanding, the required voltage for the power devices that they use, has been increasing continuously. So the high voltage market is developing due to the demand of the 'Green Technology' market and nuclear technology supports the development of those markets. By 2020 the total high voltage power devices/modules market will double. As mentioned before, a clear trend towards increased demand for high resistivity material is expected in the near future. This demand does not seem to penalize the demand for 'lower' resistivity material.

4.1 Wind-turbines

Wind-turbine electrical power generators make use of Insulated Gate Bipolar Transistors, or abbreviated, IGBT's. This component is used in power convertors with megawatt output. The variable frequency of the generator is transformed in a fixed frequency used on the electricity grid.

4.2 Solar panels

Solar panels depend on invertors that transform the direct current (DC) of the solar cells to alternating current (AC) to deliver electricity for household use or for the grid.

4.3 Hydropower

The electronic components used in the electricity generating system of the extremely powerful 'Three Gorges Dam', that was constructed in China and became operational in 2009, are state-of-the-art high voltage, high current IGBT's (6.5 kV, 1500 A) and thyristors (8.5 kV, 2500 A). This is a perfect example of components that can only be made by using the extremely homogeneous NTD-Silicon.

4.4 High Speed Trains

High speed trains reduce their power consumption by using brake systems that regenerate energy: the reduction in energy consumption can be up to 20%. The IGBT components used in modern solid-state systems assure that the generated current is comparable to the current on the feed line of the train.

4.5 High voltage transport lines

Long distance transmission of electricity via DC power lines, on the bottom of the see or on land, allows drastic reduction of losses when compared to AC transmission. IGBT's are at the heart of the components that perform the AC-DC conversion and vice versa.

4.6 Hybrid Electrical Vehicles (HEV)

Here energy regenerating brake systems play their role to reuse the energy as for high speed trains. Other conversion components in HEV's also make use of NTD-Silicon that has been irradiated in the BR2-reactor. As a result the 'well-to-wheel' energy-efficiency of an HEV is 34% versus some 19% for a combustion engine and this with a more than 40% reduction in CO_2 production. In 2011, the HEV-sales represented worldwide 2% of the car sales or 28 million vehicles.

5. Conclusions

The production of the highest quality of very homogeneous Silicon semi-conductors, so-called NTD-Silicon, can only be achieved by neutron irradiation of very pure Silicon crystals in research reactors.

The NTD-Silicon that is being produced has a broad field of high-tech innovative applications, many of which are oriented towards renewable energy applications. As the demand of these applications increases steadily due to 'green energy', 'low carbon emission' and 'energy conservation' societal arguments, the request for NTD-Silicon in quantity, in quality and homogeneity continuously increase.

The Belgian BR2 reactor contributes in a substantial and essential way to the World production of this semi-conductor material. BR2 has dedicated facilities, called SIDONIE and POSEIDON, that are capable of irradiating large quantities of Silicon ingots with diameters varying between 4" and 8" in diameter, in a wide range of resistivities and with high overall accuracies. Smaller diameters can be irradiated upon request.

BR1, a thermalised graphite research reactor, offers additional possibilities for high-resistivity NTD-Silicon production and is in the process of being qualified and equipped for increased use.

A European tripartite between France, the Netherlands and Belgium prepares the future for new research irradiation facilities due to future possible outphasing of existing tools in these countries. SCK•CEN has a unique and innovative project MYRRHA that will assure NTD-Silicon production from 2023 onwards.

POSTER:

LIFE SCIENCE APPLICATIONS

SELLAFIELD DOSE IMPACTS ON NON-HUMAN BIOTA

P. MCDONALD, E. LUTMAN, S. HUNAK

AMEC, Innovation Centre,

Westlakes Science and Technology Park, Moor Row, Cumbria CA24 3TP, UK

D COPPLESTONE

Biological & Environmental Sciences, School of Natural Sciences, University of Stirling,

Stirling, FK9 4LA, UK

A STEVENS

Sellafield Ltd, Sellafield,

Seascale, Cumbria CA20 1PG, UK

ABSTRACT

A new review of the Sellafield dose impacts on non-human biota has been performed, updating a previous review from 2004. The current review considered developments in published guidance, changes in designated conservation areas, targeted dose re-assessments using the new ERICA tool in conjunction with recent environmental monitoring data, and evaluated the importance of new dose guideline values/levels.

The major development affecting the non-human biota dosimetry approach since 2004 was the release of the 'state of the art' dose assessment tool ERICA in 2007. Other developments of interest include the latest ICRP recommendations and the inclusion of protection of the environment in the international Basic Safety Standards.

Of relevance to this study is the production and establishment of guideline values/levels. In ERICA, a screening value of 10 μGy h^{-1} is recommended where dose rates below this value indicate little need for further investigation. This value was derived through a more robust process than previous dose-to-biota modelling guideline values The implications of using 10 μGy h^{-1} as a screening value was considered in conjunction with the action level of 40 μGy h^{-1} used by the Environment Agency of England and Wales.

In this study it was found that the recommended Marine Conservation Zone on the Cumbria Coast provided six organism categories (with the exception of phytoplankton) with calculated dose rates between 10 and 27 μGy h^{-1}. These dose rates were derived using maximum reported activity biota concentrations in the Sellafield area between 2003 and 2010. Although these dose rates are equal or greater than the ERICA guideline value of 10 μGy h^{-1}, they are all below the Environment Agency regulatory action level of 40 μGy h^{-1}. Since the data used in this assessment have been significantly influenced by historical discharges and calculated dose rates are below 40 μGy h^{-1}, it is recommended that no further work is necessary in this area to assess the impact of current discharges. Dose rates greater than 40 μGy h^{-1} were produced for phytoplankton but there are known problems with the assessment of phytoplankton reported in the literature and this is an area of on-going research.

1. Introduction

During the early 2000s, in response to its requirements under the European Birds and Habitats Directives, the Environment Agency promoted the practice that the impact of radioactive discharges from industry on both aquatic and terrestrial non-human biota should be assessed since systems were becoming available where dose rates to non-human biota could be calculated [1],[2],[3]). In response to this, the former British Nuclear Fuels plc (now Sellafield Ltd) commissioned an impact assessment of its radioactive discharges on non-human biota in 2004 [4]. This assessment considered the impact on Natura 2000 sites of routine aerial and liquid discharges, including historical contributions from 1952 up to 2002, using activity concentrations predicted using BNFL transport models and the Environment Agency R&D128 dose to biota assessment methodology [2]. The review concluded that "no impact is considered likely to sensitive species or ecosystems as a result of authorised aerial and liquid discharges of ionising radiation from the BNFL Sellafield site" [4]. This review is now seven years old and the scientific developments made during this time now need to be considered to determine whether the conclusions from the 2004 impact assessment are still appropriate or whether significant re-working of the previous assessment is required. The review performed within this project considered the latest developments in the field of dose to non-human biota.

2. Review of non-human biota dosimetry developments

Since the impact assessment of Natura 2000 sites in the vicinity of the Sellafield site [4], there have been a number of developments that are worthy of note at the international and national level that may have an influence on the way radiological protection of the environment is considered in the UK.

2.1 International developments

2.1.1 International Commission on Radiological Protection

In their new recommendations [5], the ICRP has considered it appropriate to broaden its scope to address directly the subject of radiological protection of the environment. It has therefore included in its general aims those of: "*... preventing or reducing the frequency of deleterious radiation effects in the environment to a level where they would have a negligible impact on the maintenance of biological diversity, the conservation of species, or the health and status of natural habitats, communities, and ecosystems*". Furthermore, the Commission stated its intention to provide guidance and advice through the development of a Reference Animal and Plant (RAP) framework in light of the fact that there is currently a lack of consistency at an international level with respect to addressing environmental protection in relation to radioactivity.

In Publication 108, the Commission set out its RAP framework [6] and defined a small set of RAPs (12 in total) representing aquatic and terrestrial environments. The RAPs may be considered as analogous to the reference person that is used in human radiological protection which has been used to draw together all the scientific data on exposure, dose and biological effects. The advantage of using such a system within human radiological protection is that as new information arises, it is possible to identify any changes that will occur, not only to the specific aspect of the system, but also to the system as a whole. Consequently, it provides a mechanism for relating exposure to dose, dose to risk of radiation effects and then the consequences of any such effects. Thus the RAPs provide a similar, pragmatic basis for collating and analysing scientific data related to the effects of wildlife exposed to radiation in the environment.

In Publication 103, the Commission highlighted that it did not intend to produce a 'dose limit' for the environment [5]. However, to be able to convert our knowledge of the effects of radiation on different types of animals and plants into management decisions and/or judgements about whether radioactive discharges to the environment are likely to have an impact on the environment, some form of criteria (preferably numeric) is needed. Publication 108 [6] sets out the arguments for deriving such numeric criteria, and other researchers have considered this problem. ICRP opted, as a pragmatic approach, to consider the biological effects in terms of bands of dose and to identify one band within which certain biological effects were noted, or might be expected. They termed this band a derived consideration reference level. ICRP defined the DCRL as:

"*A DCRL can therefore be considered as a band of dose rate within which there is likely to be some chance of deleterious effects of ionising radiation occurring to individuals of that type of Reference Animal or Plant, derived from a knowledge of defined expected biological effects for that type of organism that, when considered together with other relevant information, can be used as a point of reference to optimise the level of effort expended on environmental protection, dependent upon the overall management objectives and the exposure situation*" [6].

Fig 1: The Derived Consideration Reference Level (DCRLs) for each of the ICRP's twelve Reference Animals and Plants [6].

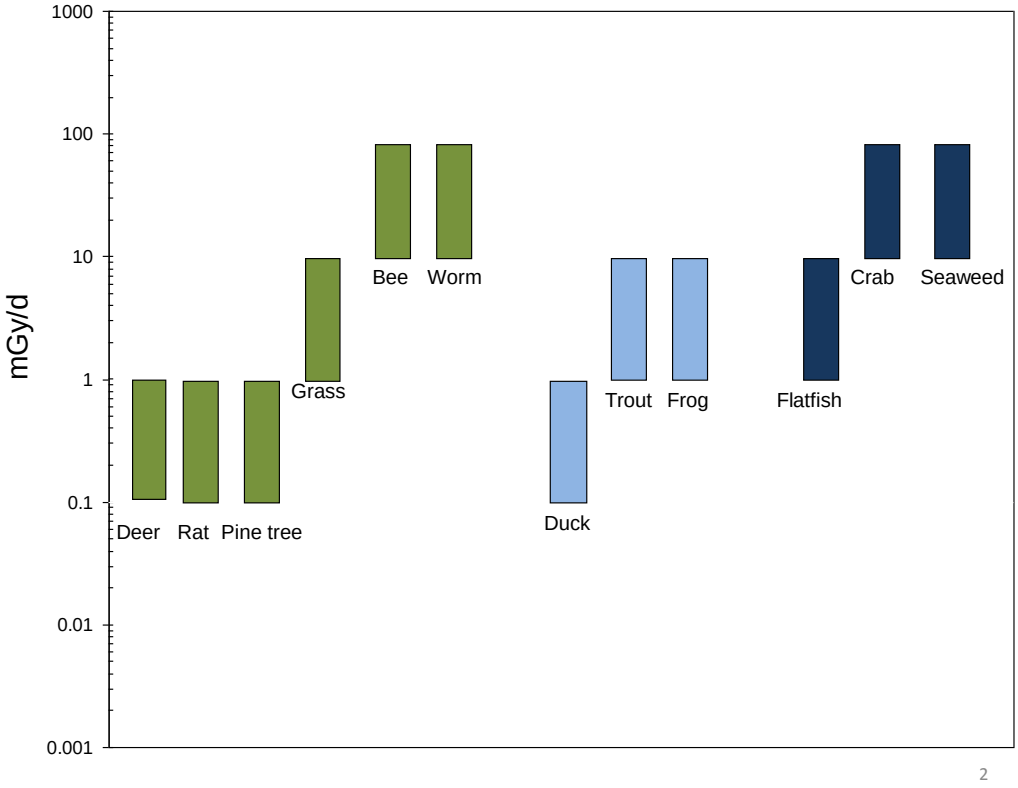

ICRP currently has a document out for consultation which describes the application of these DCRLs. For example, in a planned exposure situation, such as a proposed new nuclear power plant being built, a desired objective would be to ensure that in planning for the discharges that the dose rates to the wildlife in the area would be below the bottom of the Derived Consideration Reference Level (DCRL) band on the basis that doses that could potentially give rise to biological effects would be avoided. Bearing in mind that there may also be other sources of

radioactive substances into the environment, in reality this means that there may also need to be some 'headroom' below the bottom of the DCRL band. In the majority of cases, it is expected that the release of radionuclides are likely to be so small that exposures to both members of the public and wildlife are likely to be extremely low, although as with the habitats assessments in the UK [7], there may still be a requirement to demonstrate that this is so.

2.1.2 International Atomic Energy Agency – Environmental Modelling for Radiation Safety (I and II)

The IAEA's Environmental Modelling for Radiation Safety (EMRAS I and II) programme was launched in 2003 and was focused on areas where uncertainties remain in the predictive capability of environmental models for estimating the consequences of the releases of radionuclides to the environment. In 2004 the programme was expanded to include consideration of the impact of environmental radioactivity on non-human species. This work was conducted within the Biota Working Group (BWG) who's initial objective was to compare and validate the models being used and developed as part of the regulatory process of licensing and compliance monitoring of authorised releases of radionuclides to improve Member States' capabilities for protection of the environment.

In the BWG a total of 15 models and approaches were applied to one or more of the exercises conducted by the BWG. The models came from a number of different countries including Belgium, Canada, France, Lithuania, Russia, the UK and the USA and the participants included modellers, regulators, industry and researchers. The intercomparisons and discussions included three tools that are commonly encountered in the UK: the England and Wales Environment Agency R&D 128 [2], [3], ERICA tool [8] and RESRAD-BIOTA [9]. The ERICA tool is described below. R&D128 has been commonly used in the UK and was used as the basis for the Sellafield habitat assessments conducted in 2004 [4]. RESRAD-BIOTA is the tool used by US Department of Energy (DOE) for assessing doses to populations of animals and plants around DOE sites in the US. All three tools are freely available.

The work of the BWG clearly demonstrated that the largest contribution to variability between model predictions, and comparison with available data, is the parameterisation of the models transfer components. The methods used to determine absorbed dose rate contribute relatively little to variability between model outputs.

2.2 European developments

2.1.3 EC Funded ERICA project and its' associated Assessment Tool and effects database

The ERICA (Environmental Risk from Ionising Contaminants: Assessment and Management) Assessment Tool was produced under the EU Sixth Euratom Framework programme (contract no. F16R-CT-2004-508847) and was first released in 2007. The ERICA built on the earlier FASSET (Framework for Assessment of Environmental Impact) and EPIC (Environmental Protection from Ionising Contaminants in the Arctic) projects which were supported under FP5 Euratom.

The objective of ERICA was to provide an integrated approach to scientific, managerial and societal issues concerned with the environmental effects of contaminants emitting ionising radiation, with emphasis on biota and ecosystems. The ERICA Tool [8] was the practical manifestation of the work and resulted in a software package that is freely available to download and install. The tool was first released in 2007 and has had two major updates since then. The latest version was released in June 2011. The tool is being maintained by a subset of the original 15 ERICA consortium organisations. There is now a European FP7 Euratom funded

network of excellence (STAR – Strategy for Allied Radioecology) which is taking the lead in maintaining the ERICA tool.

The ERICA Tool implements a tiered approach to guide assessment, risk characterisation and managerial decisions including interactions with stakeholders. The Tool implements the ERICA Integrated Approach which is described in D-ERICA [10]. There are three tiers which build in complexity, data and resource requirements as you pass through the tiers (from 1 to 3). Tier 1 is a very simple conservative assessment which compares media concentrations measured or modelled for the assessment with pre-calculated environmental media concentration limits (EMCLs) that correspond to the activity concentration needed in the media (air, sediment, soil or water) that would give rise to the predicted no effect dose rate (PNEDR) which has been used to set a screening level below which there is no concern about potential impact on the environment. Tier 2 is a more refined assessment which can calculate dose rates to different wildlife groups, include additional radionuclides and modify many of the parameters that are used in the ERICA tool. The results from tier 2 are compared directly to the PNEDR (in dose rate μGy h^{-1}). Tier 3 introduces a probabilistic capability to the tool that allows the probability of specified dose rates to be estimated.

The ERICA Tool is widely regarded to be one of the two state of the art models (the other being the US RESRAD-BIOTA tool). There are clear differences in the functionality of the two main tools but the ERICA Tool is commonly being used within Europe for radiological assessments of the environment.

2.1.4 EC Funded PROTECT project

After the ERICA project was completed, the EC EURATOM Framework 6 funded PROTECT project (FI6R036425) set out to develop dose rate thresholds for wildlife to help to determine the risk of exposure to ionising radiation between 2007 and 2008. Without such criteria any radiological protection framework for the environment cannot be applied usefully in a regulatory context (e.g. for generic screening tools). The PROTECT consortium consisted of five organisations: Centre for Ecology & Hydrology (UK), Environment Agency (England and Wales), IRSN (France), Norwegian Radiation Protection Authority (Norway) and the Swedish Radiation Safety Authority (Sweden). The PROTECT project consulted with a number of stakeholders including the IAEA, EC, regulators, industry, non-government organisations and experts in chemical risk assessment.

Within the PROTECT project, the methodology outlined within the EC Technical Guidance Document on risk assessment for chemical substances [11] was used. The aim was to identify the most sensitive reproductive endpoint for any given species (cytogenetic effects were excluded) and then to use these data in a species sensitivity distribution (SSD) to determine a predicted no effect dose rate (PNEDR) for use in screening assessments. In this case, because background radiation exposure was considered in all the experiments from which the biological effect data were taken, the PNEDR should be applied as an incremental (i.e. in addition to background) dose rate.

One key problem with the available numeric criteria for use in radiological environmental assessments is that they are often single values and that they fail to take into account the differences in radiosensitivity between wildlife species. This can be a particular issue where the most exposed species may not necessarily be the most radiosensitive; this has been noted in many of the initial dose assessments for wildlife. Consequently PROTECT also attempted to derive sufficient biological effects data for different wildlife ‘groups’ (e.g. mammals, birds,

reptiles etc.). However, there were insufficient data on reproductive effects alone to enable taxon specific numeric criteria to be produced. An attempt was made using a very crude segregation (vertebrates, invertebrates and plants) to determine group specific screening levels. This resulted in values of 2, 70 and 200 μGy h^{-1} for vertebrates, plants and invertebrates respectively. The vertebrate and invertebrate screening values were determined using the SSD approach but the plant value was determined using the assessment (or safety) factor approach because there were too few data to construct the SSD. There were so few data included in the derivation of all three numbers though that PROTECT advises against using the calculated group specific screening values but rather that they are used to illustrate the intent if more relevant biological effect data can be obtained.

PROTECT returned to the derivation of a single screening value for use in a tiered risk assessment which could be applied to all species. Using different, more relevant, biological endpoint data than was included in the ERICA evaluation, PROTECT derived 22 reproductive relevant values (4 plant, 2 annelid, 3 crustacean, 2 mollusc, 2 bird, 4 fish and 3 mammal) for inclusion in a generic (all species) Species Sensitivity Distribution (SSD). The constructed SSD gave a hazardous dose rate at 5% (HDR_5) of 17 μGy h^{-1}. Given the much more thorough review of the input data and in line with the approach given in the TGD [11], a safety factor of 2 was applied to the HDR_5 and the resultant PNEDR (when rounded up) came to 10 μGy h^{-1} which happened to be the same as that derived in ERICA using a less rigorous approach for the input data selection.

2.3 UK developments

The UK has a duty to comply with the European directives on Habitats (92/43/EEC) and Wild Birds (79/409/EEC), which are administered by the UK's environmental protection agencies - the Environment Agency in England and Wales and the SEPA in Scotland. The Directives were introduced into UK legislation by the Conservation (Natural Habitats & Conservation.) Regulations 1994. Under the Habitats Regulations, the Environment Agency in England and Wales and SEPA in Scotland has obligations to review relevant existing authorisations, permits, consents, licences and permissions (collectively referred to as permits) to ensure that no Environment Agency authorised activity or permission results in an adverse effect, either directly or indirectly, on the integrity of Natura 2000 sites. In addition, the Environment Agency is also required to ensure that any new or varied permits do not have an adverse effect on the integrity of the Natura 2000 sites. In light of this, the Environment Agency, (in conjunction with Natural England and the Countryside Council for Wales) has agreed a regulatory action dose rate threshold of 40 μGy h^{-1}, based on the following:

- The FASSET project [12] indicated that there appear to be no significant adverse effects in biota exposed at levels of up to 100 μGy h^{-1};
- Work within the FASSET project [13] indicated that wildlife might receive up to 60 μGy h^{-1} from natural sources in European ecosystems; and,
- The threshold of 40 μGy h^{-1} for authorised discharges of radioactive substances is the difference between these two values.

Allott et al. [7] describes the overall process followed in England and Wales and the key findings from the assessment of the authorised radioactive discharges. The assessments involved the calculation of dose rates to organisms in 429 Natura 2000 sites in England and Wales using the R&D 128 methodology [2], [3], taking account of the combined impact of current discharges from multiple authorised releases and cautiously assuming that the discharges occur at the authorisation limits.

The total dose rate to the worst affected reference organism was less than the 40 μGy h^{-1} for all but two Natura 2000 sites (Ribble and Alt Estuaries Special Protection Areas [SPAs] and Drigg Coast Special Area of Conservation [SAC]). The calculated total dose rate to the worst affected organism for the Ribble and Alt Estuaries SAC was 520 μGy h^{-1}. This was significantly in excess of the agreed threshold and so this Natura 2000 site was included in Stage 4 of the Habitats Regulations implementation process [7].

3. Review of other developments

The location and extent of the protected Natura 2000 sites in the vicinity (up to 50 km for liquid discharges and 15 km for aerial discharges) of Sellafield have not changed since 2004 with the exception of some proposed marine sites. In September 2011, documentation was released describing recommended Marine Conservation Zones [14], [15]. This documentation referred to recommended zones within the Irish Sea region. The four 'new' zones of interest are 'The Mud Hole' (21 km off the coast of Cumbria), 'West of Walney' (8 km from Walney Island), 'Allonby Bay' (from high water mark to approx. 5.5km offshore) and 'Cumbria Coast' (extends 27 km from just north of St Bees Head south to the Ravenglass estuary) were therefore identified as requiring assessment (section 5).

4. Non-human biota dose re-assessments in recommended Marine Conservation Zones (rMCZ)

Targeted dose assessments have been performed for biota in the four zones of interest described below.

4.1 rMCZ 1 The Mud Hole

The 'Mud Hole' data have been used in ERICA to calculate the total dose rates given in Table 1. The highest calculated dose rate was 2.2 μGy h^{-1} for phytoplankton. The calculated dose rate values are below the current ERICA screening value of 10 μGy h^{-1} and the current Environment Agency regulatory action of 40 μGy h^{-1} signifying that the calculated dose rates are not significant.

4.2 rMCZ 2 West of Walney

The 'West of Walney' data have been used in ERICA to calculate the total dose rates given in Table 1. The highest calculated dose rate was 3.7 μGy h^{-1} for phytoplankton. The calculated dose rate values are below the current ERICA screening value of 10 μGy $h^{-1}$and the current Environment Agency regulatory action of 40 μGy h^{-1}signifying that the calculated dose rates are not significant.

4.3 rMCZ 10 Allonby Bay

The Allonby Bay data have been used in ERICA to calculate the total dose rates given in Table 1. The highest calculated dose rate was 42 μGy h^{-1} for phytoplankton with the next highest value being 4.6 μGy h^{-1} for polychaete worms. The value for phytoplankton is above the current ERICA screening value of 10 μGy h^{-1} and the current Environment Agency regulatory action level of 40 μGy h^{-1} signifying that further investigation may be required at this site. However, the occurrence of phytoplankton being the most exposed organism but one of the more radioresistant types of organism during other dose to non-human biota investigations has been observed leading to recommendations that the ERICA assessment methodology for phytoplankton should be re-assessed with field or laboratory data [7]. The ERICA Tool relates the phytoplankton concentration ratio (CR) closely to the Distribution Coefficient (K_d) which is

normally used to indicate a radionuclide's ability to bind to particulate/mineralogical material rather than to biological material.

4.4 rMCZ 11 Cumbria Coast

The 'Cumbria Coast' data have been used in ERICA to calculate the total dose rates given in Table 1. There are several calculated total dose rates that are greater than the ERICA screening value of 10 μGy h^{-1}. These are phytoplankton (192 μGy h^{-1}), polychaete worm (27 μGy h^{-1}), macroalgae (23 μGy h^{-1}), vascular plant (21 μGy h^{-1}), sea anemones or true corals – colony and polyp (17 to 19 μGy h^{-1}) and benthic mollusc (10 μGy h^{-1}). Issues with phytoplankton screening dose values within ERICA have been highlighted above in Section 5.3. All of these calculated dose rates, with the exception of phytoplankton, are still below the Environment Agency regulatory action level of 40 μGy h^{-1}. Since several calculated dose rates are greater than the ERICA screening value, there may be some justification in keeping this region under review.

Organism	rMCZ 1 Mud Hole	rMCZ 2 West of Walney	rMCZ 10 Allonby	rMCZ 11 Cumbria Coast
(Wading) Bird	-	-	-	0.2
Benthic fish	0.1	0.1	2.3	7.9
Benthic mollusc	0.2	0.1	1.4	**10**
Crustacean	0.5	0.02	3.1	7.0
Macroalgae	0.7	0.1	0.7	**23**
Mammal	0.01	0.01	0.05	0.3
Pelagic fish	0.06	0.1	0.8	0.1
Phytoplankton	2.2	3.7	**42**	**192**
Polychaete worm	0.6	0.1	4.6	**27**
Reptile	0.01	0.01	0.06	0.3
Sea anemones or true corals - colony	0.5	0.1	1.9	**17**
Sea anemones or true corals - polyp	0.5	0.1	2.8	**19**
Vascular plant	0.7	0.1	2.4	**21**
Zooplankton	0.1	0.2	2.0	4.1

Highlighted values indicate total dose rate per organism that equal or exceed the ERICA screening level of 10 μGy h^{-1}.

Tab 1: Calculated total dose rates [μGy h^{-1}] to reference organisms at rMCZ close to Cumbria, Northwest England.

The data used for this targeted re-assessment were the maximum reported values from annual Sellafield monitoring reports and RIFE reports [16], [17]. These data (with the exception of radionuclides with a half life of less than a few years) reflect environmental conditions resulting from a combination of recent and historical discharges. Normal practice in assessing the impact of discharges on non-human biota [7] is to use current (authorised) discharge values. Hence the re-assessment performed here, because of the influence by historical discharge practices can be considered a conservative assessment. Because of the historical discharge contributions to external dose, we propose that where dose rates exceed 10 μGy h^{-1} no further work is necessary if the overall dose remains below 40 μGy h^{-1} and where the influence of historic discharges on non-human biota activity concentrations can be shown to be significant. Also, if doses are calculated to be over 40 μGy h^{-1} then many avenues should be considered to improve the assessment, the first of which being the contribution of past discharges to dose. If

such considerations do not provide reasons for the calculated doses to be above 40 μGy h^{-1} then potentially regulatory action may take place.

The major radionuclide contributors to the calculated marine dose rates were ^{60}Co, ^{99}Tc, ^{239}Pu and ^{241}Am. Future discharges from Sellafield are predicted to decrease compared to current discharges (Sellafield Effluent Management Strategy, GEN-3223A, December 2011, Sellafield Ltd). It is anticipated therefore that by 2020 any future impacts on wildlife will be lower than they are from current authorised discharges from the Sellafield site.

5. Discussion

The main aim of this review was to determine whether the conclusions from the 2004 dose impact assessment [4] are still valid. Since 2004, significant advances in the field of dose to non-human biota have been made, and because of this, this update review takes advantage of such progress. Since 2004, the ERICA Tool has been developed and made freely available; the ICRP are establishing the use of RAPs within the overall system of radiological protection and the IAEA have continually supported the progress of model development in this field through their EMRAS programmes.

The major points to be taken from the targeted re-assessments are:

- A Tier 2 ERICA screening assessment on Recommended Marine Conservation Zones 1, 2 and 10 did not produce calculated dose rates that would warrant more attention being given to these areas. The highest calculated dose rate was 42 μGy h^{-1} for phytoplankton. It is known that the assessment approach for phytoplankton requires attention within the ERICA Tool to provide more realistic, rather than overly conservative, dose rates and that, as an organism type, phytoplankton is more radioresistant which also needs to be considered during an assessment
- The rMCZ 11 Cumbria Coast site provided six organism categories (not including phytoplankton at 192 μGy h^{-1}) with calculated dose rates between 10 and 27 μGy h^{-1}.
- These dose rates were derived using maximum reported activity biota concentrations in the Sellafield area by Sellafield Ltd and RIFE between 2003 and 2010. Although these dose rates are equal or greater than the ERICA screening value of 10 μGy h^{-1} they are all below the Environment Agency regulatory action level of 40 μGy h^{-1}. Since the data used in this assessment have been significantly influenced by historical discharges and calculated dose rates are below 40 μGy h^{-1}, it is recommended that no further assessment is necessary in this area.

6. Acknowledgement

AMEC and the University of Stirling acknowledge the Sellafield Ltd funding on behalf of NDA for this project.

7. References

[1]. Identification of candidate reference organisms from a radiation exposure pathways perspective. Framework for the Assessment of Environmental Impact. Available on-line at www.fasset.org. FASSET, 2001.

[2]. Copplestone D., Bielby S., Jones S.R., Patton D., Daniel P. and Gize I. (2001) Impact Assessment of Ionising Radiation on Wildlife. Environment Agency R&D Publication 128. ISBN: 1 85705590 X pp222

[3]. Copplestone, D., Wood M.D., Bielby S., Jones S.R., Vives J. and Beresford N.A. (2003) Habitats Regulations for Stage 3 Assessments: Radioactive Substances Authorisations. Environment Agency R&D Technical Report P3-101/SP1a. pp100

[4]. Marshall, W., Punt, K., Johnson, C., Gleizon, P. and Lutman, E. (2006). Impact assessment of the aerial and marine discharges of ionising radiation from BNFL Sellafield on Natura 2000 sites. Westlakes Scientific Consulting Ltd Report No. 030124/01 Second Issue, pp109.

[5]. The 2007 Recommendations of the International Commission on Radiological Protection. ICRP Publication 103. Ann. ICRP 37 (2-4).

[6]. Environmental Protection - the Concept and Use of Reference Animals and Plants. ICRP Publication 108. Ann. ICRP 38 (4-6).

[7]. Allott, R., Copplestone, D., Merrill, P. and Oliver, S. (2009). Habitats assessment for radioactive substances. Better Regulation Science Programme, Science Report SC060083/SR1. pp187.

[8]. Brown, J.E., Alfonso, B., Avila, R., Beresford, N.A., Copplestone, D., Pröhl, G., Ulanovsky A. (2008). The ERICA Tool. J. Environ. Radioact., 99, 1371-1383.

[9]. A Graded approach for evaluating radiation doses to aquatic and terrestrial biota. Technical standard DOE-STD-1153-2002, Modules 1-3, United States Department of Energy, Washington D.C.

[10]. Beresford N.A., Brown J.E., Copplestone D., Garnier-Laplace J., Howard B.J., Larsson C-M., Oughton D., Proehl G. and Zinger I. (2007) D-ERICA: An Integrated Approach to the Assessment and Management of Environmental Risks from Ionising Radiation. EC Project Contract No FI6R-CT-2004-508847 pp82.

[11]. Technical Guidance Document in Support of Commission Directive 93/67/EEC on Risk Assessment for New Notified Substances and Commission Regulation (EC) No. 1488/94 on Risk Assessment for Existing Substances. Luxembourg: Office for Official Publication of the European Communities.

[12]. Larsson, C-M., Jones,C., Gomez-Ros, J.M. and Zinger, I. 2004. Deliverable 6: Framework for Assessment of Environmental Impact of Ionising Radiation in Major European Ecosystems, 74pp. Framework for Assessment of Environmental Impact (FASSET) Project EC Contract No. FIGE-CT-2000-00102.

[13]. Brown, J.E., Jones, S.R., Saxén, R., Thørring, H. and Vives i Batlle, J. 2004. Radiation doses to aquatic organisms from natural radionuclides. *Journal of Radiological Protection* 24, A63–A77.

[14]. Final recommendations Summary. Irish Sea Conservation Zones, c/o Envirolink, Birchwood, Warrington, p37, 2011.

[15]. Final recommendations for Marine Conservation Zones in the Irish Sea (Submitted to the UK Government 31st August 2011). Irish Sea Conservation Zones, c/o Envirolink, Birchwood, Warrington, p435, 2011.

[16]. Monitoring our Environment. Discharges and Monitoring in the UK, British Nuclear Group Sellafield Ltd, Annual Reports 2003 - 2005 and Sellafield Ltd, Annual Reports 2006 – 2010.

[17]. RIFE 9 – 16. Environment Agency, Food Standards Agency, Northern Ireland Environment Agency, Scottish Environmental Protection Agency (2004-2011). Radioactivity in Food and the Environment.

Gene expression changes in mouse fetal fibroblasts after chronic exposure to simulated space conditions

Michaël Beck[1,2], Marjan Moreels[1], Roel Quintens[1], Khalil Abou-El-Ardat[1,2], Kevin Tabury[1], Arlette Michaux[1], Ann Janssen[1], Mieke Neefs[1], Patrick Van Oostveldt[2,3], Winnok H. De Vos[2,3], Sarah Baatout[1,2].

[1]*Laboratory of Molecular and Cellular Biology, Institute for Environment, Health and Safety, Belgian Nuclear Research Centre, SCK•CEN, Mol, Belgium*
[2]*Department for Molecular Biotechnology, Ghent University, Ghent, Belgium*
[3]*NB-photonics, Ghent University, Ghent, Belgium*

ABSTRACT

Space conditions including microgravity and cosmic radiation are difficult to simulate on Earth. However, ground-based models exist to simulate space flight conditions including irradiation (IR) facilities and µg simulating devices such as the Random Positioning Machine (RPM). In the present study, a space simulating experimental model was used to monitor gene expression changes in primary skin fibroblasts obtained from mouse fetus. Cells were continuously exposed (65h) to a low dose (55mSv) IR mixture of neutrons and γ-rays and/or simulated microgravity (RPM), after which whole genome microarrays were performed. Two different analytical methods to detect changes in gene expression were used in parallel in this study including 'single gene analysis' and 'Gene Set Enrichment Analysis'.
Our results show that simulated microgravity affected fetal murine fibroblasts by inducing oxidative stress responsive genes and decreasing the expression of genes involved in cytoskeleton remodeling. Similarly, chronic exposure to low dose IR caused a down-regulation of genes involved in cytoskeleton pathways, but also in genes involved in cell cycle regulation and DNA damage response. Many of the genes or gene sets that were altered in the individual treatments (RPM or IR) were not significantly changed in the combined treatment (RPM and IR), indicating no synergistic effect between RPM and IR.

1. Introduction

Although many studies have reported a proper development in space-flown animals upon return to Earth, other studies have shown various spaceflight-induced physiological and morphological alterations at critical steps of the development (for reviews, see ref. [1, 2]). Among the deleterious conditions for living organisms found in space, microgravity has clearly been linked to developmental complications in mammals and amphibians [3]. Less is known about the impact of cosmic radiation on development, although it is a well-known risk factor for astronauts during spaceflight [4]. Moreover, animal studies on Earth have shown that ionizing radiation can have a detrimental impact on embryonic development [5-7].

In the present study, an *in vitro* model system was used in which primary cultures of fetal fibroblasts of murine origin (PFC) were chronically exposed (65) to simulated space conditions (microgravity and/or radiation) to assess changes in gene expression. For microgravity simulation, we used the Random Positioning Machine (RPM) which is one of the most widely used instruments and which has proven valuable in many cell types [8-11]. As far as cosmic radiation is concerned, simulating the wide variety of ions ranging from low to very high energies encountered in space is problematic, especially if irradiation is combined with microgravity simulation models. In fact, there is no facility to date offering the possibility to produce chronic exposures of very high-energy beams consisting of multiple charged particles. We therefore chose to use a source of californium (Cf) -252 for low dose-rate chronic exposure consisting of a mixture of high LET neutrons and low LET γ-rays.

The important amount of data generated with a high-throughput technology such as microarrays constitutes a double-edged sword: it allows us to take a snapshot of the whole

expression pattern, but extracting the relevant information out of it is challenging [12, 13]. To overcome this problem, analysis tools have been developed, such as single gene statistical analysis methods that are widely used to determine the differentially expressed genes and Gene Set Enrichment Analysis (GSEA) which aims at identifying gene expression differences in groups of genes acting synergistically in a cellular process [13]. Both analytical methods were used in parallel in this study.

2. Materials and methods

Cell culture. BALB/cJ Rj (Janvier Laboratories, France) fetuses originating from 2 different litters were dissected 17 days *post conception*. Their skin was harvested and mechanically and enzymatically dissociated. The obtained cell suspension was subsequently centrifuged for 10 min at 350 g, solubilized in F12 medium (Invitrogen) supplemented with 20% FBS and 1% penicillin / streptomycin (Invitrogen) and seeded in 6-well plates, one fetus skin in each well. The cells were allowed to grow for up to 3 or 4 passages at 37°C (5% CO_2) and were subsequently frozen in FBS with 10% dimethyl sulfoxide (Sigma-Aldrich, USA). The primary cultures were thereafter thawed and allowed to grow for two weeks. Cells were seeded at a density of 10^5 cells in 12.5cm² flasks and allowed to adhere for 24 h before treatment.

Simulation of space conditions. Chronic exposure (65 h) to simulated space conditions included microgravity simulation using the desktop Random Positioning Machine (RPM, Dutch Space, Leiden, The Netherlands) and irradiation. Four treatment conditions were defined: controls (CTRL), microgravity simulation (RPM), irradiated (IR) and a combination of both (RPM&IR). The flasks were completely filled with medium, sealed and placed on the RPM at a rotational velocity between 55°/s and 65°/s. Direction, speed and interval were set as random. Controls were placed in the same incubator. For chronic low dose irradiation, cells were exposed to a mixture of neutrons (98.2%) and γ-rays (1.8%) directly or indirectly originating from a Cf-252 source placed at 4.13 m from the incubator. The dosimetry was performed with bubble detectors as previously described [14] for neutron irradiation and with 600 cc ionization chamber (NE) coupled with a Farmer electrometer for γ-rays. The total dose received was 55.94 ± 19.70 mSv (862 µSv/h), which approximately corresponds to 35 times the dose rate measured on the International Space Station (ISS) [15], a total dose corresponding roughly to a stay of 100 days in the ISS.

Total RNA isolation, Affymetrix microarrays and data analysis. Total RNA was isolated according to the manufacturer's instructions using Qiagen kit (Qiagen, Venlo, The Netherlands). After labeling samples were hybridized to Affymetrix Human Gene 1.0 ST Array chips (Affymetrix, Santa Clara, USA). The RNA was treated using the GeneChip WT cDNA Synthesis and Amplification Kit (Affymetrix, Santa Clara, USA) according to the manufacturer's instructions. The resulting RNA was hybridized onto Affymetrix Mouse Gene 1.0 ST Arrays.

Raw data (.cel-files) were imported at exon level in Partek Genomics Suite v6.5 (Partek Incorporated, USA). Briefly, robust Multi-array Average (RMA) background correction was applied, data were normalized by Quantile Normalization and probe set summarization was performed by Median Polish method. Gene summarization was performed using one-step Tukey's biweight method. These data were either further analyzed with the Partek Genomics Suite software for single gene analysis and by the GSEA software (v2.0, BROAD Institute of Harvard and MIT, USA). For single gene method, a 4-way ANOVA, taking into consideration the scan date (which also consists in the litter), the fetus, the gender and the treatment as factors, was performed to determine which genes had a significantly altered expression between different conditions. For pathway analysis, Kegg and PathART databases were interrogated with ArrayTrack v3.3.0 (National Center for Toxicological Research, USA).
For the GSEA, a selection of 144 gene sets from Gene Ontology (GO) databases were interrogated. Gene sets were considered to be significantly differently regulated with a False Discovery Rate (FDR) q value <0.05.

3. Results

Single gene analysis revealed that 119 genes were down-regulated and 55 genes were up-regulated by more than 1.5 fold change (unadjusted p-value <0.01) across all treatments (Fig. 1). Kegg and PathART databases indicated that the 54 genes that were down-regulated specifically by RPM treatment were mostly involved in cell cycle regulation (p53 and p21 mediated pathways), in cytoskeleton modeling, cell junctions and cell signaling via integrins, IL1, and TGF-β. Within the list of individual genes that were specifically down-regulated after IR or RPM&IR treatments, no clear pathway was found. On the other hand, in the 52 genes that were up-regulated upon RPM and RPM&IR treatments, interleukin signaling (IL11 and MMP) and glutathione metabolism were the most prominent pathways affected. Some genes were differentially expressed by RPM and RPM&IR, but only a few genes were common between IR and RPM&IR.

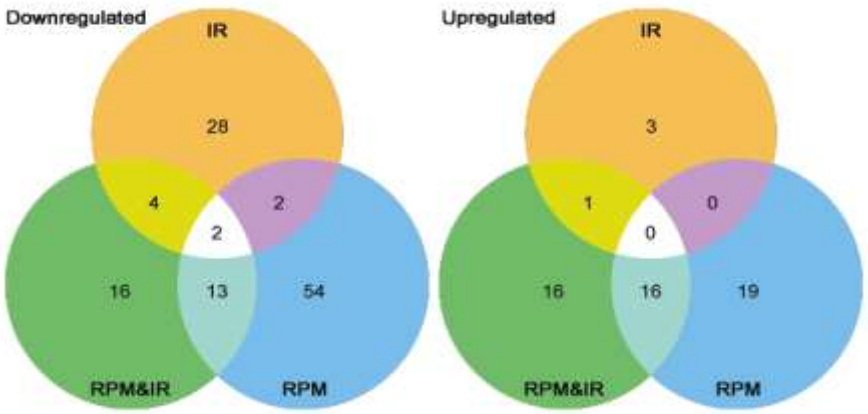

Figure 1. Venn diagram showing the number of down-regulated (left) or up-regulated (right) genes in mouse fetal fibroblasts upon one of the three space simulation treatments (p<0.01, fold change > 1.5): chronic exposure to low dose of irradiation (IR), simulated microgravity (RPM), or the combination of both (RPM&IR).

In contrast to the results obtained by single gene analysis, GSEA revealed a high impact of IR on coordinately differentially expressed genes. Indeed, a total of 63 gene sets were significantly down-regulated after chronic low dose irradiation. Among them, 30 were exclusively enriched in irradiated samples (Fig. 2), although this number may be an overestimation due to redundancy between gene sets. The gene sets that were specifically down-regulated after irradiation conditions are mostly involved in DNA damage response, cell signaling, cell cycle, RNA processing and protein turnover. Moreover, we detected in all treatments some significantly down-regulated gene sets involved in cell signaling, cell cycle, transcription, protein turnover, cell shape, adhesion, motility and communication. To note, two gene sets involved in oxidative phosphorylation were significantly down-regulated solely in RPM&IR samples. No gene set was significantly up-regulated in any of the treatments.

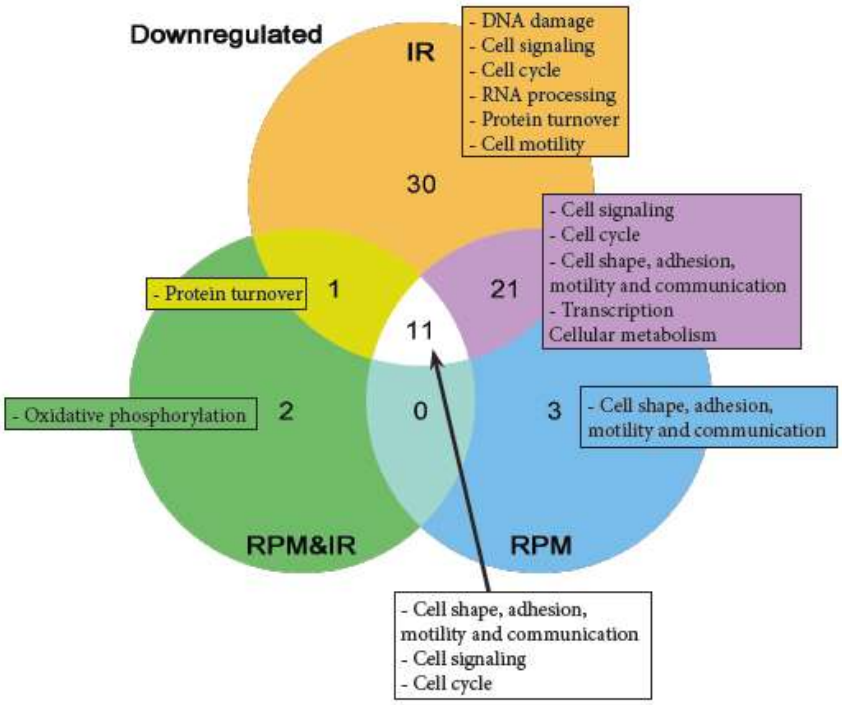

Figure 2. Venn diagram showing the number of gene sets significantly down-regulated in mouse fetal fibroblasts upon one of the three space simulation treatments: chronic exposure to low dose of irradiation (IR), simulated microgravity (RPM), or the combination of both (RPM&IR). Boxes include the cellular pathways in which these gene sets are involved.

4. Discussion and conclusion

Single gene method analysis revealed a significant impact of 65 h of simulated microgravity on gene expression of murine fetal fibroblasts. The combination of RPM&IR triggered a differential expression of fewer genes than RPM alone. Only a few genes had an altered expression in IR samples, suggesting that such a low dose of radiation had a moderate impact on gene expression.

Among the up-regulated genes upon RPM treatment, several of them are involved in the glutathione metabolism (*Gsta1, Gsta2* and *Gclm*). We also report an up-regulation of the heme oxygenase 1 (*Hmox1*), a cytoprotective enzyme against oxidative stress. Notably, these genes are targets of the nuclear factor-erythroid 2 p45-related factor 2 (Nrf2) which induces transcription of cytoprotective genes containing antioxidant response elements [16]. Since simulated microgravity has already been linked to oxidative stress generation [17-19], it is not surprising to observe an up-regulation of anti-oxidant genes.

As far as the down-regulated genes are concerned after RPM treatment, four genes are involved in the cytoskeleton (*Actg2*, *Acta1*, *Cnn1* and *Fhl1*). Interestingly, these four genes were shown to be regulated by the serum response factor (SRF), possibly mediated by the Rho signaling [20]. Rho signaling is believed to be an important pathway for focal adhesion assembly and cytoskeleton remodeling in response to cellular tension stress [21]. Moreover, it is hypothesized to play a role in microgravity response [18]. Furthermore, Rho GTPases activities were shown to be increased in dermal fibroblasts subjected to simulated microgravity for 30 and 120 min, thereafter decreasing to reach similar values as controls at 48 h of treatment [22].

At the gene set level, GSEA did not detect any up-regulation, except for the structural constituents of the ribosome in IR-treated samples. Among the 63 significantly down-regulated gene sets, 30 were specifically enriched in IR-treated samples. These IR induced gene sets are involved in DNA damage response, cell signaling, cell cycle, RNA processing,

protein turnover or cell motility. However, various other gene sets involved in the same cellular processes, except for the DNA damage response, were also enriched in RPM and RPM&IR treatments. Many of them were involved in cell signaling, among which Rho and Ras GTPases, inositol and phosphatidylinositol, JNK and insulin receptor-mediated pathways. The down-regulation of these signaling pathways may lead to an alteration of the cell cycle [23]. In addition to its major role in the cellular response to radiation [24, 25], the regulation of the cell cycle has been previously shown to be affected by simulated microgravity as well [26]. GSEA revealed that gene sets involved in the positive regulation of the cell cycle were down-regulated in all treatments. However, upon IR, cells displayed a significant down-regulation of gene sets involved in cell cycle arrest, indicating no trend towards a pro- or anti-proliferative expression profile.

Many gene sets involved in the composition of the cytoskeleton (actin and microtubule) and inter- (cell junctions) and extracellular connections (extracellular matrix) were affected by all treatments. While it has been shown in various cell types that cytoskeleton remodeling starts promptly upon simulated microgravity or real microgravity treatments [18, 27-29], few studies investigated the effects of ionizing radiation on the cytoskeleton. Interestingly, gene sets involved in integrin and receptor binding were specifically down-regulated upon RPM. Our data confirm therefore that integrins play a significant role in the cellular response to simulated microgravity.

Changes in DNA damage responsive gene sets were detected only in IR and not in RPM&IR-treated cells. As it is unlikely that the movement of the RPM was able to prevent DNA damage from occurring. We suggest that simulated microgravity decreased DNA damage signaling. The hypothesis that cells subjected to microgravity might tolerate moderate DNA damage has already been proposed in order to conciliate the discrepancy between data showing higher radiosensitivity or, on the contrary, the absence of effects under microgravity [30], although no microgravity-driven alteration of DNA repair kinetics after high doses of X-rays has been measured on space-flown human fibroblasts [31].

In conclusion, this study shows that chronic exposure to simulated microgravity affects fetal murine fibroblasts, especially at the single gene level, by increasing the expression of oxidative stress response genes and decreasing the expression of genes involved in cytoskeleton remodeling. As far as irradiation is concerned, we detected a decrease in expression of gene sets involved in cytoskeleton mechanisms, in cell cycle and DNA damage response after a chronic low dose-rate irradiation. Our results indicate that the effects of the combination of the two treatments did not result in a synergism between the two separate effects, since many altered genes or gene sets in RPM or IR were not detected in RPM&IR. We also show that the combination of a single gene method coupled to a GSEA allows the identification of both significant changes in specific genes and in subset of genes acting in the same pathways.

5. References

1. Clément, G. and K. Slenzka, *Fundamentals of space biology: research on cells, animals, and plants in space*. 2006: Microcosm.
2. Ronca, A.E., *Mammalian development in space.* Adv Space Biol Med, 2003. **9**: p. 217-51.
3. Crawford-Young, S.J., *Effects of microgravity on cell cytoskeleton and embryogenesis.* Int J Dev Biol, 2006. **50**(2-3): p. 183-91.
4. Cucinotta, F.A., M.-H.Y. Kim, and L. Ren, *Evaluating shielding effectiveness for reducing space radiation cancer risks.* Radiation Measurements, 2006. **41**(9-10): p. 1173-1185.
5. Jacquet, P., *Sensitivity of germ cells and embryos to ionizing radiation.* J Biol Regul Homeost Agents, 2004. **18**(2): p. 106-14.
6. ICRP, *Pregnancy and medical radiation. ICRP Publication 84*, in *Annals of the ICRP*. 2000.
7. UNSCEAR, *Report to the General Assembly with Annexes*. 1986, United Nations Scientific Committee on the Effects of Atomic Radiation (UNSCEAR): New York.

8. van Loon, J.J.W.A., *Some history and use of the random positioning machine, RPM, in gravity related research.* Advances in Space Research, 2007. **39**(7): p. 1161-1165.
9. Borst, A. and J. van Loon, *Technology and Developments for the Random Positioning Machine, RPM.* Microgravity Science and Technology, 2009. **21**(4): p. 287-292.
10. Villa, A., et al., *Cell behavior in simulated microgravity: a comparison of results obtained with RWV and RPM.* Gravit Space Biol Bull, 2005. **18**(2): p. 89-90.
11. Grimm, D., et al., *Different responsiveness of endothelial cells to vascular endothelial growth factor and basic fibroblast growth factor added to culture media under gravity and simulated microgravity.* Tissue Eng Part A, 2010. **16**(5): p. 1559-73.
12. Shi, J. and M.G. Walker, *Gene Set Enrichment Analysis (GSEA) for Interpreting Gene Expression Profiles.* Current Bioinformatics, 2007. **2**(2): p. 133-137.
13. Subramanian, A., et al., *Gene set enrichment analysis: a knowledge-based approach for interpreting genome-wide expression profiles.* Proc Natl Acad Sci U S A, 2005. **102**(43): p. 15545-50.
14. Vanhavere, F., et al., *A combined use of the BD-PND and BDT bubble detectors in neutron dosimetry.* Radiation Measurements, 1998. **29**(5): p. 573-577.
15. Cucinotta, F.A., et al., *Physical and biological organ dosimetry analysis for international space station astronauts.* Radiat Res, 2008. **170**(1): p. 127-38.
16. Hayes, J.D. and M. McMahon, *NRF2 and KEAP1 mutations: permanent activation of an adaptive response in cancer.* Trends Biochem Sci, 2009. **34**(4): p. 176-88.
17. Wang, J., et al., *Simulated microgravity promotes cellular senescence via oxidant stress in rat PC12 cells.* Neurochem Int, 2009. **55**(7): p. 710-6.
18. Nikawa, T., et al., *Skeletal muscle gene expression in space-flown rats.* FASEB J, 2004. **18**(3): p. 522-4.
19. Liu, Y. and E. Wang, *Transcriptional analysis of normal human fibroblast responses to microgravity stress.* Genomics Proteomics Bioinformatics, 2008. **6**(1): p. 29-41.
20. Beamish, J.A., et al., *Molecular regulation of contractile smooth muscle cell phenotype: implications for vascular tissue engineering.* Tissue Eng Part B Rev, 2010. **16**(5): p. 467-91.
21. Ingber, D.E., *Tensegrity II. How structural networks influence cellular information processing networks.* J Cell Sci, 2003. **116**(Pt 8): p. 1397-408.
22. Loesberg, W.A., et al., *Simulated microgravity activates MAPK pathways in fibroblasts cultured on microgrooved surface topography.* Cell Motil Cytoskeleton, 2008. **65**(2): p. 116-29.
23. Hall, A., *Rho GTPases and the control of cell behaviour.* Biochem Soc Trans, 2005. **33**(Pt 5): p. 891-5.
24. Jeggo, P., *The role of the DNA damage response mechanisms after low-dose radiation exposure and a consideration of potentially sensitive individuals.* Radiat Res, 2010. **174**(6): p. 825-32.
25. Jeggo, P. and M.F. Lavin, *Cellular radiosensitivity: how much better do we understand it?* Int J Radiat Biol, 2009. **85**(12): p. 1061-81.
26. Grimm, D., et al., *How and why does the proteome respond to microgravity?* Expert Rev Proteomics, 2011. **8**(1): p. 13-27.
27. Meloni, M.A., et al., *Cytoskeleton changes and impaired motility of monocytes at modelled low gravity.* Protoplasma, 2006. **229**(2-4): p. 243-9.
28. Servotte, S., et al., *Establishment of stable human fibroblast cell lines constitutively expressing active Rho-GTPases.* Protoplasma, 2006. **229**(2-4): p. 215-20.
29. Nichols, H.L., N. Zhang, and X. Wen, *Proteomics and genomics of microgravity.* Physiol Genomics, 2006. **26**(3): p. 163-71.
30. Manti, L., *Does reduced gravity alter cellular response to ionizing radiation?* Radiat Environ Biophys, 2006. **45**(1): p. 1-8.
31. Horneck, G., et al., *DNA repair in microgravity: studies on bacteria and mammalian cells in the experiments REPAIR and KINETICS.* J Biotechnol, 1996. **47**(2-3): p. 99-112.

6. Acknowledgements

This research is performed in the context of the ESA Topical Team on "Developmental Biology in Vertebrates" and has been/is financially supported by the following PRODEX/ESA contracts (C90-303, C90-380, C90-391 and 42-000-90-380).

European Nuclear Society
Rue Belliard 65
1040 Brussels, Belgium
Telephone: +32 2 505 30 50 - FAX: +32 2 502 39 02
enc2012@euronuclear.org
www.enc-2012.org